Deglacial sequences and glacio-isostatic adjustment: Quaternary compared with Ordovician glaciations

Pierre Dietrich, Jean-François Ghienne, Patrick Lajeunesse, Alexandre Normandeau, Rémy Deschamps, Philippe Razin

Deglacial sequences and glacio-isostatic adjustement: Quaternary compared with Ordovician glaciations

Pierre Dietrich[1,2]*, J.-F. Ghienne[1], P. Lajeunesse[3], A. Normandeau[4], R. Deschamps[5], & P. Razin[6]

[1] Institut de Physique du Globe de Strasbourg (UMR 7516), Ecole et Observatoire des Sciences de la Terre, Université de Strasbourg/CNRS, France

[2] Department of Geology, University of Johannesburg, Johannesburg, South Africa

[3] Université Laval, Québec, Canada

[4] Geological Survey of Canada – Atlantic, Dartmouth, Nova Scotia, Canada

[5] Institut Français du Pétrole-Energie Nouvelle, Rueil-Malmaison, France

[6] ENSEGID, Institut Polytechnique de Bordeaux, Pessac, France

(*pdietrich@uj.ac.za)

Abstract

Deglacial sedimentary sequences recording the decay and final demise of ice sheets result from intricate interactions between the pattern of ice margin retreat, inherited basin physiography and relative sea-level (RSL) changes. A specific emphasis is here given to the glacio-isostatic adjustement (GIA), which may force postglacial local RSL fall in spite of concomitant glacio-eustatic rise. In this contribution, we characterize a Quaternary deglacial succession emplaced in such a setting, subsequently used as an analogue to interpret an end-Ordovician deglacial record. The Quaternary deglacial succession, tens of meters thick, formed under condition of RSL fall forced by the GIA in *ca.* 10,000 years in the aftermath of the deglaciation. This sedimentary succession consists of a lower, fining-upward sequence representing the backstepping of ice-contact depocenters following the retreat of the ice margin, and an upper, coarsening-upward sequence that relates to the subsequent progradation of a glaciofluvial delta system. A very similar stratigraphic stacking pattern characterizes the Ordovician analogue, suggesting a comparable deglacial sequence. By analogy with the Quaternary succession, this ancient deglacial record would have hence been emplaced under conditions of RSL fall forced by the GIA. Moreover, it must only represent a very short time interval that could be viewed as virtually instantaneous regarding the Late Ordovician glaciation. Such a vision is at odds with commonly accepted interpretations for such successions.

Keywords: Deglaciation, isostatic rebound, forced regression, Quaternary, Québec, Ordovician, Morocco, Glaciomarine, Delta.

Although ice ages have occurred repeatedly throughout the Earth history, the reconstruction of related glaciation scenarios has remained an issue for geologists and palaeoclimatologists. In sedimentary archives, the identification of glacial surfaces such as striated pavements provides diagnostic features when unravelling development of past ice sheets through time and space (Deynoux & Ghienne, 2004; Le Heron *et al.* 2005; Dowdeswell *et al.* 2007; Denis *et al.* 2009; Moreau & Ghienne, 2016). A correct understanding of intervening depositional successions is, nevertheless, also required. Glaciogenic facies such as glaciomarine diamictites, tillites or outwash-fan sandstones potentially offer relatively straightforward interpretations (Eyles & Eyles, 1992; Ghienne *et al.* 2010; Hirst, 2012; Le Heron, 2012). In contrast, associated sedimentary successions that do not display apparent glacial signature, such as fluvial, shallow-marine or turbidites may threat a correct interpretation as they are commonly interpreted as non-glaciogenic. Their overall depositional context may, however, still relate to glacially-influenced systems when characterized, for instance, by outstanding rates of sediment supply or by rapid and important relative sea-level (RSL) changes. In particular, the interpretation of thick (> 50 m) shallowing-upward sequences made up of apparently non-glaciogenic deposits within an overall glaciation-related succession is challenging as they may be, in the absence of high-resolution (<1000 yr) chronostratigraphic framework, individually interpreted as the result of either (i) a glacio-eustatically driven sea-level fall associated to an ice-sheet growth; (ii) a highstand progradation during an interglacial episode; or (iii) a glacio-isostatically driven RSL fall succeeding a glacial retreat. Progradation tied to a glacio-isostatic adjustement, which the present contribution focuses on, is typically achieved over short periods of time (<20 000 years) after a deglaciation and characterized by unusual rates of RSL fall initially reaching 10 $cm.year^{-1}$. A correct interpretation of sedimentary processes associated with isostatically-forced RSL fall is hence crucial in unravelling ice thickness and spatial extent of past ice sheets, commonly well-known in the Quaternary but barely constrained for ancient glacial episodes (e.g., Creveling *et al.* 2016). The same is true for transgressive trends, some of which might relate counterintuitively to major ice-sheet advances in the case of a proglacial glacio-isostatic lithospheric flexure (Dunbar *et al.* 2008; Stocchi *et al.* 2013).

Field-based case studies and numerical stratigraphic modelling have recently demonstrated that forced-regressive deposits have preservation potential in depositional successions (Strong & Paola, 2008; Holbrook & Bhattacharya, 2012). Glacio-isostatically forced pro- to postglacial suites should then be an essential component of deglacial sequences (Boulton, 1990; Corner, 2006; Shaw *et al.* 2008; Eilertsen *et al.* 2011; Storms *et al.* 2012; Hein *et al.* 2014; Nutz *et al.* 2015; Zecchin *et al.* 2015; Dietrich *et al.* 2017a), even if such records remain uncommonly recognised in the deep-time glacial record (e.g., Haldorsen *et al.* 2001; Pazos, 2002; Ghienne, 2003; Le Heron *et al.* 2006; Creveling *et al.* 2016; Mottin et al., 2017). In this contribution, we take advantage of offshore geophysical data

(Lajeunesse *et al.* this volume) combined with onshore facies analyses and LiDAR imagery from the Québec North Shore (eastern Canada, Fig. 1) to build up a time-calibrated, more than 50 km long, geometrically well-constrained sequence stratigraphic model that may serve as a benchmark for a better understanding of deglacial sequences in the deep time. We then confront a particular end-Ordovician glaciation-related sequence of southern Morocco (central Anti-Atlas) with this Late Pleistocene to Holocene record, interpreting the former in the light of the latter. We finally discuss the implications of such an analogy.

The glacio-isostatic adjustement and associated RSL changes

The glacio-isostatic adjustement (GIA) is a key phenomena associated with deglaciation, taking place as soon as the ice begins to thin in a given area and continuing during postglacial times well after the final ice-sheet withdrawal. The GIA is a viscoelastic process (Kearey *et al.* 2009; Watts, 2009) implying a rapid uplift of the lithosphere, which outstanding amplitudes (several tens to hundreds of meters), rates (up to 10 cm per year) and timing (<20 000 years) are without equivalent amongst other geological processes (Sella *et al.* 2007; Koohzare *et al.* 2008; Tarasov *et al.* 2012).

The GIA directly results from deglaciation; it is therefore concomitant to a global glacio-eustatic sea level rise essentially induced by the release of large quantities of meltwater in the ocean (Tamisiea & Mitrovica, 2011; Lambeck *et al.* 2012; Creveling & Mitrovica, 2014; Peltier *et al.* 2015). At a regional scale, glacio-eustatic sea level rise competes with glacio-isostatic RSL fall; the dominant process being mainly determined by the geographic position relative to the former maximum extent of the ice margin and by the timing of its retreat (Fig. 2; for a conceptual model of RSL variation forced by GIA, see Boulton, 1990). Regarding continental-scale ice-cover recessions in phase with global deglaciation —the Laurentide Ice Sheet (LIS) for the last Late Pleistocene-aged deglaciation— and in depositional area located close to the maximal extent of the former ice-sheet margins, the initial pattern of RSL is controlled by the GIA, as initial rates of glacio-eustatic sea level rise are minor, resulting in RSL fall. Later, increasing rates of glacio-eustatic sea level rise outpace the decreasing rates of GIA-induced RSL fall. In such an area, the eustatically-dominated zone of Boulton (1990), the deglacial RSL curve hence shows an initial, short-term, relatively high-amplitude fall followed by a moderate rise (curve 1 in Fig. 2; e.g., Hein *et al.* 2014). In contrast, in areas formerly covered by significant ice thicknesses, in central parts of the ice mass but also in the extensive areas located relatively far inside (> 100's km) the maximum ice front extent, the GIA remains the dominant process controlling RSL throughout the deglacial evolution. Such a prevalence leads to a continuous and significant (> 100 m) RSL fall effective since the onset of ice-free conditions and up to thousands of years after full deglaciation (curve 2 in Fig. 2: isostatically-dominated zones). In coastal areas, this has

a profound impact on the stratigraphic architecture of deglacial sequences (Fig. 2; Boulton, 1990; Zecchin *et al.* 2015; Dietrich *et al.* 2017a).

Deglacial sequences: the Québec North Shore perspective

Geological and deglacial setting

Our Late Pleistocene to Holocene analogue is located on the Québec North Shore (Fig. 1, North Shore of the Gulf of the St. Lawrence, eastern Canada). Onshore, the hilly bedrock is characterized by deep (100-400 m) and steep-flanked structural valleys, 0.5-3 km in width, incised prior the last glacial period (see Lajeunesse, 2014), and in which modern rivers flows. Offshore, the Laurentian Channel is a deep (>300 m) and long (>1500 km), partly fault-bounded trough bordered to the north by a 0-20 km wide coastal shelf (Duchesne *et al.* 2010; Pinet *et al.* 2016). Along the proximal reaches of the shelf, at the outlets of the structural valleys, thick (>100 m) Late Pleistocene to Holocene raised sediment bodies expose prominent morphosedimentary structures (moraines, outwash channels, beach ridges, abandoned meanders; Dredge, 1983; Dionne and Occhietti, 1996; Dyke, 2000; Bernatchez, 2003; Occhietti, 2007; Dietrich *et al.* 2017a; 2017b). At first glance, related depocenters correspond to conventional river deltas affected by forced regression driven by the GIA (Hart and Long, 1996; Shaw *et al.* 2002; 2006). However, recent studies have concluded that (i) in most cases, ice-contact depositional systems (subaqueous ice-contact fans and ice-contact deltas) emplaced at the mouth of the structural valleys have significantly contributed to the initial construction of these so-called "deltaic" bodies (Dietrich *et al.* 2016a; 2017a; Gagnon-Poiret *et al.* in press); (ii) extensive complexes of subaqueous grounding-zone wedges (GZWs) and grounding line fans have been identified throughout the coastal shelf (Lajeunesse, 2016; Lajeunesse *et al.* this volume); (iii) deltaic depocenters, initially confined in the structural valleys but subsequently emerging on the open coast, were essentially fed by glacial meltwater and glaciogenic sediments (glaciofluvial deltas; Dietrich *et al.* 2017a; Normandeau *et al.* 2017), and (iv) delta-front channels or canyons are today essentially inactive, their abandonment being dated back to the retreat of the ice-margin out of the river drainage basins (Normandeau *et al.* 2015; 2017). Therefore, a continuum of depositional systems is identified in the deltaic complexes —rather than deltas— of the Québec North Shore, these sediment bodies being essentially deglacial relicts incorporating ice-contact deposits and glaciofluvial deltas.

Following the Last Glacial Maximum (LGM, *ca.* 23 ka ago, Shaw *et al.* 2006), during which the LIS margin reached the edge of the continental platform, the ice initially retreated mainly by calving up to stabilization on the Québec North Shore (Shaw *et al.* 2002; 2006; Occhietti *et al.* 2011; Stokes *et al.* 2015). From *ca.* 12-10 ka onward, the grounding of the LIS margin became terrestrial and pursued an ablation-dominated ice-front recession toward the hinterland. The postglacial Goldthwait Sea

submerged the glacio-isostatically flexured lowlands after the glacial retreat, the local RSL reaching a maximum elevation of *ca.* 150 m.a.s.l. in the study area (marine limit, see Shaw *et al.* 2002; 2006; Dietrich *et al.* 2016a; 2017a). As the bottom of most the structural valleys is lower than the marine limit, they formed fjords in the aftermath of ice retreat from the coastal area. Meltwater and glaciogenic sediment discharge delivered by the retreating ice margin and carried by proglacial rivers fed coastal glaciofluvial deltas affected by rapid RSL fall owing to the active GIA (1-10 cm.year^{-1}, Shaw *et al.* 2006; Tarasov *et al.* 2012; Peltier *et al.* 2015). The connection between the glaciofluvial deltas and the LIS margins ceased between 10 to 6 ka, depending on the northward extent of the drainage basins as the ice margin retreated from them (Normandeau *et al.* 2017; Dietrich *et al.* 2017b). Ensuing sedimentation essentially reflected a paraglacial development which took place under slower rates of RSL fall. Nowadays, the RSL in the Estuary and Gulf of the St. Lawrence is approximatively stable; the still ongoing GIA in this region (Sella et al., 2007; Koohzare et al., 2008) being essentially compensated by modern global eustatic rise (Woodworth et al., 2011). Modern-day river-derived sediment load is minimal and shallow-marine reworking processes are predominant along the delta shorelines.

Anatomy of a deltaic complex

The morphostratigraphic record of such a deltaic complex, the so-called Sept-Îles deltaic complex, is described below in order to illustrate palaeo-environmental changes and stacking pattern of related depositional units since the onset of the deglaciation around 13-11 ka cal BP (calibrated kilo-years Before Present, see Reimer *et al.* 2009) (Figs 1 and 2). The stratigraphic architectures of other deltaic complexes have been described in detail in Dietrich *et al.* (2017a; see also fig. 4b for an outline).

Deposits that constitute the large (*ca.* 900 km², Fig. 3) Sept-Îles deltaic complex were documented both onshore and offshore (Figs 1 and 3). Onshore deposits consist of glacio-isostatically raised sedimentary terrains emplaced at the outlet of the deep, narrow and steep-flanked structural valley in which the modern Moisie River flows. Deltaic lobes, beaches and sandspits as well as a moraine known as the Lake Daigle Moraine have long been identified (Dubois, 1979; Dredge, 1983; Drapeau, 1992; Hein *et al.* 1993; Bernatchez & Dubois, 2004) and are easily recognizable on LiDAR data (Fig. 3). The offshore counterpart comprises an irregular seafloor characterized by a prominent relief, partly buried by ice-contact —grounding zone wedges and fans—, glaciomarine, glaciofluvial and paraglacial sediments tied to the last deglaciation (Fig. 3; Syvitski & Praeg, 1989; Josenhans & Lehmann, 1999; St. Onge *et al.* 2008; Normandeau *et al.* 2013; Lajeunesse *et al.* 2013; Boyer-Villemaire *et al.* 2013; Lajeunesse, 2016; Lajeunesse *et al.* 2007; 2013; this volume; Pinet *et al.* 2016). Figure 4 synthetises the stratigraphic architecture of this deltaic complex under the form of a geometrically-constrained, dip-oriented transect running through 50 km from far offshore (180-200 m b.s.l., Fig. 3)

up to the foothills of the uncovered basement (170 m a.s.l.). Onshore and offshore depocenters described below from south (lowest part) to north (highest elevation) are correlated on the basis of radiocarbon dating and cross-cutting stratigraphic relationships. Oldest deposits (12 500 ± 40 years Cal BP, GZW1, Lajeunesse & St-Onge, 2013) are those found at the southern edge of the transect while the youngest, the presently active depositional systems, stand in its exact middle, in relation with the coastal shelf (Normandeau *et al.* 2013). Deposits that stand at the northern end of the transect, the Lake Daigle Moraine, are intermediate in age (*ca.* 10.8 cal ka BP, Occhietti et al., 2008).

The transect (Fig. 4) begins at its southern edge with distinctive sediment bodies representing subaqueous grounding zone wedges (GZWs) draped by glaciomarine and postglacial muds (see details in Lajeunesse *et al.* this volume). Upslope, an actively prograding coastal shelf fed by longshore drift downlaps onto the glaciomarine deposits (Normandeau *et al.* 2013).

Onshore, two stepped deltaic lobes, which correlative delta plains lay at 40 and 60 m.a.s.l., represent the most voluminous sediment package of the deltaic complex (Fig. 3). These two stepped lobes have a comparable well-defined tripartite offlapping stratigraphic architecture comprising lower delta slope, upper delta slope and delta plain/delta front deposits (Fig. 5A). The 10 m-thick lower delta slope deposits consists of gently-sloped (<1°) seaward-dipping foresets containing normally-graded sand beds interpreted as the result of turbidity flows. Contorted beds, either slump or large-scale load structures are frequently interstratified (Fig. 5B). The upper delta slope consists of steeper (mean 4-5°), concave-upward clinothems, with mean heights and lengths of 8-10 m and 130-150 m, respectively (Fig. 5A). The clinothems are composed of stacked normally-graded sand beds composed of medium- to fine-grained sand draped by mm-scale silt laminae, interpreted as deposited by turbidity flows. Coarsening- and thickening-upward trend evidences the deltaic progradation. The overlying delta front and delta plain deposits consist of a 4-8 m thick erosion-based gravelly sandsheet lying on delta slope deposits. The lower part of the sandsheet consists of well-sorted fine-grained sand characterized by mm-scale, sub-horizontal, well-defined laminae highlighted by heavy minerals alternating with trains of fine-grained wave- and combined- rippled sand and trough cross-strata. These deposits are ascribed to a delta-front shoreface. Gravelly coarse-grained planar and trough cross-stratified sands of the upper part represent braided-stream deposits (Fig. 5C). Depositional facies —braided delta plain and turbiditic sand lobes—, gravitational instabilities and significant progradation rates inferred from radiocarbon datings (Fig. 4), together highlight an active delta built up and point out for a glaciofluvial deltaic system fed by glaciogenic sediment supply. The inferred deltaic depositional profile, involving a subhorizontal shoreface connecting downslope to concave-upward foresets suggests mixed-influenced delta clinoforms (compound clinoforms of Swenson *et al.* 2005), with a delta brink (rollover point) positioned at the transition between the shoreface and the delta slope (subaqueous delta

clinoform *sensu* Patruno *et al.* 2015). Depositional bathymetries can be inferred on the basis of sigmoid-shaped clinoform height; a fair estimate of the depth of the lower to upper delta slope transition being *ca.* 15 m.

At higher elevation, an ice-contact, Gilbert-type delta which has its topset beds at 135 m.a.s.l. has been identified immediately basinward of a spillway breaching the Lake Daigle moraine (Dietrich *et al.* 2016a). Delta topset beds consist of trough cross-stratified conglomeratic sand and steep foresets include backstepping cross-strata interpreted as cyclic steps. Both the ice-contact Gilbert delta and the moraine overlie slightly older, poorly-exposed, sand-prone foreset beds which the radial dips nevertheless draw a fan shape in plan view (Fig. 3). Along their upper segments, these foreset beds consist of a crude alternation of rippled silty fine-grained to cross-stratified or massive very coarse-grained sand including lonestones up to the boulder size (Fig. 5D). Beds are contorted or disrupted, showing dense networks of downstepping extensional fractures, especially beneath lonestones, and small-scale folds. In places, foreset deposits are overlain by an up to 2 m-thick sandy, boulder-rich diamicton (Fig. 5D). Shear deformation at its lower contact suggests a subglacial till (Evans *et al.* 2006). In the absence of topset beds, the overall architecture is thus interpreted as a subaqueous ice-contact fan (Lønne, 1995; Occhietti, 1997). The till cover and the moraine ridge indicate a glacier re-advance on the fan, best interpreted as an autocyclic process rather than as a climatically-controlled event; the prograde-aggradation of the subaqueous ice-contact fan and the hence reduced water depth having permitted the grounding and re-advance of the ice front (Boulton, 1990; Brinkerhoff et al., 2017). In terms of ice margin dynamic, this subaqueous ice-contact fan is put on an equal term to the GZWs observed offshore, namely a stillstand/re-advance in the general ice retreat trend and thus refers to a grounding zone sediment body (Lajeunesse *et al.* this volume). The transition from the subaqueous fan to the overlying Gilbert delta marks the demise of marine ice fronts and the onset of deltaic sedimentation in the study area, the Gilbert delta corresponding to the oldest deglacial depositional system that was adjusted to RSL.

Glaciomarine muds are observed draping the bedrock and underlying other younger deposits throughout the study area. These muds (Fig. 4) consist of well-laminated argillaceous silts containing abundant shell debris and sparse, well-rounded, up to pebble-sized ice rafted debris (IRD). These muds represent tens of meters of accumulation conformably burying antecedent topographies of the bedrock up to 120 m a.s.l. (Dredge, 1983). Glaciomarine muds were mainly deposited by settling process from turbid buoyant meltwater plumes. The surface bounding the glaciomarine muds below and the sand-sized offlapping deltaic lobe deposits above encompasses in places a hiatus of 2600 years (from 10.8 to 8.2 ka) as shown by radiocarbon dates (Fig. 4).

The emerging counterpart of the Sept-Îles deltaic complex is marked throughout by entrenched river meanders, resulting in severe downcutting of all the aforementioned deposits. In

addition, raised and stepped beach deposits made up of well-sorted sand and heavy mineral placers characterize the basinward edge of the lowest deltaic lobe (Figs 3 and 4).

Deltaic complexes: a three-staged deglacial sequence

Based upon the Sept-Îles case study, as well as upon other deltaic complexes analysed along the Québec North Shore (e.g., Duchesne *et al.* 2010; Normandeau *et al.* 2017; Dietrich et al., 2017a; 2017b), a generic model encompassing the entire deglacial evolution is here proposed, distinguishing three stages of development (Fig. 6). The thickness of the resulting deglacial sequence, the duration of which is in a few thousands of years, exceeds in places 100 m (Fig. 7; see also Dietrich *et al.* 2017a). Note, however, that although this sedimentation model is generic for most of the deltaic complexes of the Québec North Shore, given ages are valid for the Sept-Îles case study only, each other systems having specific timing inferences (Dietrich *et al.* 2017b).

The first stage is characterized by the deposition of backstepping glaciomarine depocenters punctuating the recession of the ice-sheet margin. These depocenters correspond to grounding zone sediment bodies emplaced during short-term stillstands in the order of a few hundred years (Lajeunesse and St. Onge, 2013; Lajeunesse, 2016; Lajeunesse *et al.* this volume). The turnaround from a glaciomarine to a continental ice front, recorded by the transition from the subaqueous ice-contact fan to the ice-contact Gilbert delta, is here interpreted as an autogenic process controlled by interactions between RSL fall, inherited topography and sediment aggradation (*e.g.,* Powell, 1990). Of mainly local significance, this event cannot be correlated along the Québec North Shore (Shaw *et al.* 2002).

The second stage is tied to the emplacement of glaciofluvial deltaic lobes that developped when the ice margin retreated from its stillstanding position toward the hinterland and fed glaciogenic supplies to the coast. Initially confined in valleys (fjords), glaciofluvial deltas rapidly prograded on the coast shelf. The initial in-valley delta progradation corresponded in the Sept-Îles case study to a period of sediment starvation on the main coast (from 10.8 to 8.2 ka, Fig. 6). It is virtually recorded by the hiatus that exist between the glaciomarine muds and the deltaic lobes. In the absence of sedimentary income, the now-abandoned Gilbert delta foresets were reworked by shore-related processes that deposited the highest –and then oldest– raised beach ridges. No major fluvial incision occurred during this period of glaciofluvial delta progradation in spite of coeval high rates of RSL fall (Fig. 6). High sediment discharge was responsible for a steep proglacial fluvial equilibrium profile, the slope of which was greater than the descending regressive accretionary shoreline trajectory (Leeder & Stewart, 1996; Blum *et al.* 2013; Prince & Burgess, 2014; Dietrich *et al.* 2017a). A downward shift of the lower deltaic lobe within and in front of the upper one however occurred when RSL was at 40 m a.s.l. Dated back to *ca.* 7.4 cal ka BP (Fig. 5), this shift is interpreted as the result of an autogenic process sometimes

268 referred to as *autoincision* (Muto and Steel, 2004; Swenson and Muto, 2007), as comparable facies
269 suites in both deltaic lobes point to similar depositional processes and conditions. Autoincision
270 corresponds to a period of fluvial degradation throughout a period of fluvial aggradation, both
271 occurring within a same period of steady RSL fall and sediment supply. Such a glaciodeltaic dynamic
272 was active up to the retreat of the ice margin from the drainage basin, a transition accompanied by a
273 drastic shutdown in meltwater and sediment supply. In the Sept-Îles area, this transition occurred
274 when the RSL was located at *ca.* 40 m a.s.l. and is thus dated back to 7.3 cal ka BP (Fig. 6).
275 The third stage essentially consists in a reworking of the former ice-contact and glaciofluvial
276 deposits. On one hand, rivers evolved from braided to meandering and began to incise within the
277 former deltaic deposits. On the other hand, shallow-marine processes reworked the now mostly
278 inactive glaciofluvial delta front. Both processes are interpreted as the result of a dramatic decrease
279 of the fluvial input vs. shallow-marine processes ratio, in relation with the retreat of the ice margin
280 from the drainage basin. As already recognized in other case studies, this is inferred to have a profound
281 impact on downstream depositional patterns (Church, 1972, 2006; Syvitski, 1989; Forbes & Syvitski,
282 1994; Corner, 2006; Eilertsen *et al.* 2011; Hein *et al.* 2014; Nutz *et al.* 2015; Normandeau *et al.* 2017).
283 Regarding the deltaic complexes and sedimentary development, we thus argue that this major event
284 corresponded to the onset of the paraglacial evolution, even if paraglacial conditions *stricto sensu*
285 started earlier at the scale of individual, more restricted, geomorphic systems (early vs. late paraglacial
286 evolutions of Hein *et al.* 2014).
287 To sum up, the trajectory of the successive depocenters draws a large loop characterized by
288 an early backstepping trend followed by a descending regressive trend (Fig. 6, lowest cartoon). The
289 backstepping of glaciomarine ice-contact depocenters (GZWs then subaqueous ice-contact fan)
290 reflects the successive positions of receding sediment entry points at the interface between the ice
291 margin and the seafloor. The resulting stacking pattern consists of a fining-upward sediment wedge
292 including coarsening-upward cycles of higher frequency (Fig. 7a), the latter being interpreted as the
293 expression of the individual progradation of the successive ice-contact systems. As soon as a
294 continental-based ice margin developed, corresponding in the study area to the emergence of the
295 subaqueous ice-contact fan into the ice-contact Gilbert delta, a shoreline was re-established and
296 conventional trajectory analysis (Helland-Hansen and Hampson, 2009) could applied. A low-angle,
297 accretionary descending regressive trajectory (*sensu* Helland-Hansen and Hampson, 2009)
298 characterized the emplacement of the ice-proximal to ice-distal glaciofluvial deltas, depositing a thick
299 coarsening-upward progradational suite (Fig. 7a). Forced-regressive paraglacial shallow-marine
300 deposits coeval with river entrenchment and fluvial terraces unconformably rest on the progradational
301 suite. Their onset marks the signature of the retreat of the ice margin from river drainage basin. A
302 non-accretionary, descending and regressive high-angle trajectory is noted at this time owing to

303 sediment starvation. As a result, the synthetic sedimentary log representing in 1D this loop (Fig. 7a) is
304 characterized by an initial lower fining-upward trend (backstepping glaciomarine depocenters)
305 overlain by a coarsening-upward motif (descending regressive trajectory). Although the stacking
306 pattern mimics a transgressive-highstand-falling stage cycle, the depositional suite corresponds to a
307 single deglacial sequence, which was entirely deposited in a context of continuously falling RSL. The
308 thickness, stratigraphic architecture and geographic position of such a deglacial succession along a
309 shelf profile depends on complex interactions between decreasing RSL fall rates, pattern of ice-margin
310 retreat, inherited basin physiography and sediment supply (Zecchin, 2007). In particular, the presence
311 of a relatively shallow shelf bordered by a coastal escarpment had a major influence on the location
312 and architecture of this sequence (Normandeau *et al.* 2017).

313 *Stratigraphic surfaces*

314 The sediment packages associated to the three stages of the above-described deglacial sequence are
315 bounded by three stratigraphic surfaces (Figs 7, 8 and 9): (1) a basal Glacial Surface of Erosion (GSE),
316 (2) a Glaciofluvial Transition Surface (GTS), and (3) an unconformity at the base of the paraglacial
317 deposits here referred to as the Paraglacial Transition Surface (PTS). An upper, fourth transgressive
318 surface, although not recognized along the Québec North Shore, is identified in settings where
319 postglacial RSL rise was the ultimate development of the deglacial sequence (eustatically-dominated
320 zone, Figs 2 and 9).

321 The basal glacial surface of erosion, at the interface between the bedrock —or rare pre-Late
322 Wisconsinan sediments— and glaciogenic deposits tied to the last deglaciation, essentially represents
323 subglacial erosion of the pleniglacial period (LGM). In the study area, it superimposes the glacial
324 surface of erosion and the glacial retreat surface *sensu* Zecchin *et al.* (2015). Subordinate glacial
325 surfaces lying on top of the GZWs and tied to glacial stillstand or re-advance (Lajeunesse, 2016)
326 correspond to lower-rank glacial retreat surfaces (Zecchin *et al.* 2015) (Fig. 7d). They may not be
327 correlated laterally from place to place along the Québec North Shore.

328 The glaciofluvial transition surface (GTS) bounds ice-contact deposits below —namely
329 subaqueous fan and Gilbert delta—, and glaciofluvial deltaic deposits above (Fig. 7d). This surface
330 marks the glacial retreat from the study area and is distinct (younger) from the autogenic transition
331 from a marine to a continental-based ice margin. Contrasted sedimentological signatures may
332 characterize the GTS (Fig. 8). Depending on specifics of the study site, mainly the distance from any
333 ice-contact systems, along-strike and along-dip, changes in the GTS attributes are noted. In the
334 absence of a nearby ice-contact system (distal-lateral section in figure 8), as it is precisely the case in
335 the Sept-Îles case (Fig. 7), the GTS is marked by the transition from ice-distal glaciomarine muds below
336 to the overlying, somewhat coarser-grained, deposits of the lower glaciofluvial delta slope above.

Alternatively, if the studied area is located close to an ice-contact system (proximal section in figure 8), the GTS is positioned on top of related turbiditic facies suites. It underlies comparatively finer-grained deposits of a lower delta slope. This type of facies dislocation is well-expressed in the Portneuf case study (Dietrich *et al.* 2017a; Fig. 4b). In both cases, the GTS encompasses a significant temporal hiatus in regards to the duration of the deglacial sequence, and, as such, may be intensively bioturbated. In the Sept-Îles area, this hiatus encompasses *ca.* 2600 years, which represents the delay existing between the retreat of the ice margin from the lake Daigle moraine to the subsequent deltaic progradation issuing from the structural valley (Fig. 6). Offshore, the GTS is in places highlighted by an erosion surface originating from winnowing processes and subsequently draped by thin postglacial hemipelagites (Lajeunesse *et al.* this volume).

The unconformity at the base of the shallow-marine and fluvial paraglacial deposits, the Paraglacial Transition Surface (PTS), marks the retreat of the ice margin from the drainage basin. The direct consequence of this event is the shutdown of the glaciofluvial sediment supply to the delta system, the age of which depends on the extent of the deglaciated drainage basin (Dietrich *et al.* 2017b). This surface also corresponds to the transition from an accretionary descending regressive shoreline trajectory to an essentially non-accretionary descending regressive trajectory (*sensu* Helland-Hansen & Hampson, 2009; see Dietrich *et al.* 2017a, their Fig. 10). Although specifics of the PTS may recall those of a Basal Surface of Forced Regression (BSFR, Hunt & Tucker, 1992), it must be noted that this surface has no genetic link with any trend reversal in the RSL change pattern and can occur at any time throughout the RSL fall history.

A fourth stratigraphic surface would correspond to a Transgressive Ravinement Surface (TRS). It has not been identified along the Québec North Shore but has developed in formerly glaciated areas located in the eustatically-dominated zone where a RSL rise had characterized late postglacial times (Figs 2 and 9C; Shaw *et al.* 2008; Hein *et al.* 2014; Billy *et al.* 2014). Here, such as along the Gulf of Maine or off Newfoundland, backstepping ice-contact depocenters, forced-regressive and submerged glaciofluvial deltas, refered to as 'regressive delta' in Hein *et al.* (2014), are very similar to those illustrated in this contribution. However, they had been subsequently flooded during the Holocene (Shaw *et al.* 2002; 2006). In these cases, deltaic sediment bodies are truncated by a TRS, which itself underlies a late deglacial Transgressive System Tract (TST) (Figs 2 and 9C). If the Québec North Shore has not yet experienced any significant RSL rise, it is, however, expected these deglacial sequences would be superimposed by a TRS in the case of a hypothetical flooding tied to the melting of the Antarctic ice sheets. The TRS is therefore the only stratigraphic surface of the deglacial sequence properly tied to a RSL change.

An end-Ordovician deglacial sequence in the Anti-Atlas (southern Morocco)

Stratigraphic setting

The end-Ordovician glacial record of the Anti-Atlas is part of a thick Palaeozoic succession that crops out on the northern limb of the Tindouf Basin, an epicontinental basin characterizing the northern part of the West African Craton (Fig. 10; Destombes *et al.* 1985; Boote *et al.* 1998; Burkhard *et al.* 2006). In the central Anti-Atlas, a NW-SE oriented depocenter known as the Tagounite Trough developed in the Late Ordovician (Destombes *et al.* 1985). At the basin axis, the up to 2 km thick Ordovician succession is dominated by shallow-marine siliciclastics (Fig. 11). During the Late Ordovician, immediately prior to the glaciation, offshore shales prevailed in the basin (Loi *et al.* 2010). They grade laterally towards SW and SE basin edges into sandier, shoreface to tidal facies.

The Ordovician sedimentary succession comprises the Sandbian to Late Katian Ktaoua Group and the Hirnantian Second Bani Group (Destombes *et al.* 1985). The latter is itself subdivided in the Lower and Upper Second Bani formations (Fig. 11), the lower boundary of the latter corresponding to a composite glacial surface of erosion (Fig. 12). The ice margins did not reach southern Morocco before the middle to late Hirnantian (Destombes *et al.* 1985; Sutcliffe *et al.* 2001; Bourahrouh *et al.* 2004; Loi *et al.* 2010; Ghienne *et al.* 2014) and the glacial record is thus suspected to solely corresponds to the acme of the end-Ordovician glaciation, when the ice sheet was close to the continental margin of Gondwana (Ghienne *et al.* 2007a, 2014; Le Heron and Craig, 2008). The glacial record includes soft-sediment subglacial shear zones, glaciomarine diamictites, glaciotectonic fold-and-thrust belts, tunnel valleys, periglacial deformations as in other parts of northern Africa (Destombes, 1968; Sutcliffe *et al.* 2001; Ghienne *et al.* 2007a, 2014; Le Heron, 2007, 2016; Clerc *et al.* 2013; Nutz *et al.* 2013; Ravier *et al.* 2015). Intervening fluvial, deltaic, tidal and turbiditic sandstones are also recognized, as well as offshore shales.

The study area offers a 150 km long outcrop belt known as the Jbel Bani, to the SW of the town of Zagora and at the western edge of the Tagounite Trough. Here, the Hirnantian, pre-glacial Lower Second Bani Fm. wedges out from the east to the west beneath the glacial surface of erosion that cut westward into older preglacial deposits (Fig. 11). Three informal stratigraphic units are recognized in the Upper Second Bani Formation (Fig. 13A). The lower unit is a sandstone-dominated package preserved in up to 200 m deep, NNW to WNW oriented incision/palaeovalleys. It is interpreted as the record of one or several ice sheet growth and decay episodes. The middle unit, which the present contribution focuses on, is bounded by a glacial surface of erosion below and a transgressive ravinement surface above. As detailed in the following, this middle unit is itself subdivided into two vertically superimposed subunits of regional extent: a glaciomarine wedge below and a deltaic wedge above. Together, they form a succession reaching 140 m in thickness that wedges out against the basal glacial surface of erosion. The third upper unit unconformably overlying the middle one corresponds

405 to a relatively thin, cross-stratified sandstone-dominated unit. It is succeeded by Silurian strata, which
406 are characterized by bioturbated siltstones and black shales, yet a stratigraphic hiatus is usually
407 identified (Destombes *et al.* 1985; Lüning *et al.* 2000; Nutz *et al.* 2013).

408 *Ice-sheet configuration*

409 The glacial surface at the base of the middle unit cut either into preglacial deposits (Lower Second Bani
410 Fm. or Ktaoua Group) or into the lower unit sandstones (Figs 11 and 12). Considering the upper
411 bounding surface of the upper unit as a datum, thickness changes of the middle unit essentially reflect
412 glacial erosion depths. Thickness changes and limited indications for ice flows (grooves, striae, glacial
413 lineations, Fig. 10) are compatible with a large trough, *ca.* 50 km in width, 100-150 in depth, and at
414 least 150 km long, which would be oriented NNW-SSE. A push structure associated with a pebble
415 lodged on a glacial pavement (Fig. 14a) suggests that ice was essentially flowing ESE-wards, i.e., toward
416 the Tagounite Trough axis. This unexpected ice flow orientation regarding a NW-ward flowing End-
417 Ordovician ice sheet at the regional scale is however indirectly substantiated by (i) a glaciotectonic
418 fold-and-thrust belt, known further 100 km to the east, corroborating local ice flows from the west (Le
419 Heron, 2007; Dietrich *et al.* 2016b); (ii) underlying clinothems indicating NE-ward to eastward
420 preglacial depositional dips and progradation trends (Fig. 11). The eastern part of the study area where
421 the middle unit is thin to absent would represent the interfluve domain.

422 *The glaciomarine wedge*

423 The lower part of the middle unit (lower subunit) is up to 75 m in thickness and consists at first-order
424 of a fining-upward succession. It shows a superimposition of 5-35 m thick facies sequences, most often
425 displaying coarsening- and thickening-upward trends with subordinate fining-upward evolutions (Figs
426 12 and 13a). Glacial surfaces have been recurrently inferred owing to deformed deposits at the top of
427 coarsening-upward facies sequences. In most cases, inferred glacial surfaces are smoothed by ripples
428 trains, concealing any potential subglacial shear structures. Either relatively thick argillaceous intervals
429 including sandstone beds (Fig. 14b) or sandstone bed packages with subordinate, thin argillaceous
430 intervals are recognized. Argillaceous intervals grade from sand-free siltstones to muddy, structureless
431 fine-grained sandstones, frequently including dispersed quartz granules and gravel- to boulder-sized
432 intraclasts (sandstone clast, sandy pseudo-nodules), and more rarely extrabasinal clasts (e.g., granites,
433 Fig. 14d). Deformed, 1-10 m wide, sandstones masses, lenses or beds are frequent within the
434 argillaceous intervals. Interestingly, intra- and extra-basinal clasts observed in argillaceous facies are
435 absent in the sandstones. Load casts are common and some sand intrusions (dykes) have also been
436 observed. Intercalated tabular or lenticular sandstone beds (<1 m thick) are usually medium-grained,
437 though coarse-grained to granular facies may occur in places, especially as infill of m-scale gutter to

channel forms. Sandstone bed packages are 2-10 m in thickness. In most cases, medium-grained sandstones are well sorted, hindering the identification of primary sedimentary structures. Horizontal to subhorizontal laminations, however, seem to prevail, oblique cross-strata are rare. Undulating laminations with 1-2 m wavelength have been recurrently suspected, possibly representing climbing dune cross stratification (CDCS: Ghienne *et al.* 2010). Rip-up clasts are frequent, commonly highlighting lag deposits. Vertical sheet dewatering structures occur in places. Assemblages of sub- to super-critical climbing ripples have been observed in a single 5 m-thick sandstone body (Fig. 14c). They differ from common climbing ripple assemblages by the presence of conformable 1-5 mm-thick clay drapes along the aggrading ripple bedforms.

Overall, this sediment wedge onlapping a glacial surface of erosion and including fine-grained intervals with outsized extrabasinal clasts interpreted as IRD (dropstones) is associated with a glaciomarine environment. Deposition from buoyant plumes is inferred for siltstone-dominated to argillaceous sandy facies, representing ice-distal to ice-proximal settings, respectively. Sandstones were essentially derived from dilute to hyperconcentrated sediment-laden underflows, either filling in channel forms or expanding laterally (tabular bed sets). The underflows may relate to ice-distal turbiditic lobes (i.e., isolated bed) and/or a jet-efflux model in front of subglacial conduits issuing at groundling lines (relatively thick bed package), the latter configuration being necessary in subaqueous environments to assure high rates of sand fallout at the origin of CDCS (Ghienne *et al*. 2010; Hirst, 2012; see discussion in Girard *et al*. 2015). The coarser grained facies, circumscribed to small-scale channel or gullies, are interpreted as the downslope remobilization of ice-contact sediment wedges during high-magnitude events. Climbing ripples including clay drapes suggest modulation of subglacial outflows by tidal processes or discharges with diurnal rhythmicity. The overall fining-upward trend formed by successive and superimposed coarsening-upward facies sequences is interpreted as the result of backstepping glaciomarine depositional systems highlighting the early stage of a punctuated deglacial sequence. The proposed sequence-stratigraphic correlation (Fig. 12) identifies up to six glaciomarine depositional bodies. The thicker and sandier bodies probably referred to as grounding zone sediment body, as suggested by poorly defined glacial surfaces atop some of the coarsening-upward facies sequence. The other, less developed bodies may be ascribed to immature or distal portions of grounding zone sediment bodies not involving a glacial re-advance.

The deltaic wedge

The upper part of the middle unit (upper subunit), varying between 5 and 50 m in thickness, conformably overlies the glaciomarine subunit (Figs 12 and 13). Its base is marked by a well-defined facies dislocation owing to the occurrence of the finer-grained deposits (shaly siltstones), the

disappearance of ice-rafted debris and the initial predominance of ripple and climbing ripple cross-stratification in sandstone deposits. Thinly bedded heterolitic deposits displaying starved ripples in m-thick facies successions are observed in places (Fig. 14e). Load casts are ubiquitous and slump structures that remobilize former rippled sands are frequent. Above is a thickening-upward succession, within which cross-strata prevail in stacked, m-scale, medium-grained sandstone beds (Fig. 13b). Tangential cross-strata are predominant, commonly including lags of small rip-up clasts. Planar cross-strata and subhorizontal lamination showing parting lineations are less frequent. Few channel structures have been identified and shallow and large-scale erosion surfaces have been observed in the westernmost section (Fig. 13b). Palaeocurrents from cross-stratal dips are not well organized, and some inversions from bed to bed have been noted. Rhythmic assemblages of thin- to thick laminations forming tangential to sigmoidal bundles are present. The uppermost horizons show a variety of sedimentary structures such as wave ripples, adhesion ripples, ice-crystal marks. Bioturbation is virtually absent. In the eastern section (interfluve domain), only the lower fine-grained interval was preserved below the erosion-based, transgressive upper unit (Fig. 12).

The upper subunit thus corresponds to a thick, shallowing-upward succession, starting with relatively deep, fine-grained sediments and terminating with subaerial sand as demonstrated by adhesion ripples and ice-crystal marks. The interval of fine-grained deposition representing a prodelta setting is better developed to the east and poorly expressed to the west. In the lower part of the succession, heterolithics with starved ripples suggest low-density turbidity flow (levées deposits?). Mass movement expressed by slump structures indicates the development of a depositional slope. The onset of active sand deposition relates to trains of ripples suggesting expanding flows in delta-slope environments. Lower-flow regime conditions prevailed upstream in the subaqueous to subaerial delta plain as demonstrated by the prevalence of megaripples and/or dunes. A tidal influence is strongly suspected (rhythmic bundles, current inversions) but is not demonstrated owing to the virtual absence of clays, only present in the form of rip-up clasts. The upper horizons of the deltaic succession originate from subaerial delta plain deposits, and occurrence of adhesion ripples indicates emergence in places. The overall succession corroborates a delta progradation. The regional setting, as well as the greater development of the prodelta/lower slope deposits to the east, together suggest an eastward to northward delta progradation, which is admittedly not so evident on the basis of palaeocurrent trends. The upper subunit thus originated from a wide depositional system, including a tidally-influenced braidplain that prograded into a relict glacial trough, initially partly infilled by the glaciomarine wedge. The absence of clear clinoformal geometries at the outcrop scale suggests relatively low-angle depositional slopes.

Relationships with the post-glacial transgressive deposits

505 The upper unit is an extensive, 5-20 m thick, sharp-based, cross-stratified sandstone sheet that overlies
506 the trough infill (middle unit) and adjacent interfluve areas (Figs 12 and 13b). Bed thicknesses are in
507 the 0.5-2 m range and compound cross-strata are commonly identified (Fig. 14f). The sandstone sheet
508 rapidly grades upwards into a (<2 m) fining- and thinning-upward succession of bioturbated, storm- to
509 wave-influenced sandstones including HCS beds, wave ripples and condensed horizons (Fig. 14g).
510 Further to the east, it includes a Hirnantia fauna, indicating a latest Ordovician age, at least in a basinal
511 position (Destombes *et al.* 1985; Sutcliffe *et al.* 2001). However, in the study area, no age data are
512 directly available. Fine-grained sandstones lying atop the cross-stratified sandstone sheet are middle
513 Rhuddanian in age (Destombes *et al.* 1985; Willefert, 1988).

514 Succeeding to the underlying delta progradation, the cross-stratified sandstones of the upper
515 unit of the Upper Second Bani Fm. are understood as a transgressive sandsheet made up of shallow-
516 marine dune sands migrating along a re-flooded basin margin (Figs 10 and 11). The upper unit is thus
517 fairly comparable to similar units in other North Gondwana, latest Ordovician post-glacial settings, all
518 of which postdating and truncating the underlying glaciation-related strata (Sutcliffe *et al.* 2001;
519 Ghienne, 2003; Ghienne *et al.* 2007b). Developed on top of the sediment wedge marking local
520 deglaciation, the transgressive sandstones are interpreted as having been emplaced during the longer-
521 term deglaciation of the North-Gondwana platform (latest Ordovician) and up to a lowermost Silurian
522 deepening event from which dunes became essentially inactive and reworked by storms (see also
523 Moreau, 2011). Final deglaciation occurred later in the Lower Silurian, inundating the platform.
524 Sedimentation receded much later with the deposition of Silurian black shales; timescale of the latter
525 evolution being in millions of years, therefore not tied to local deglaciation. A diachronous (latest
526 Ordovician to lowermost Silurian?) transgressive ravinement surface involving tidal processes is
527 interpreted from the sharp-based lower bounding surface of the upper unit, while its upper bounding
528 surface is ascribed to a lower Silurian wave ravinement surface.

529 **Discussion**

530 *The record of a deglacial sequence in the light of the Quaternary analogue*

531 Many similarities exist when comparing the Quaternary Québec North Shore succession to the Late
532 Ordovician Moroccan record (Fig. 15). Aside from the general deglacial context, the paramount
533 commonality consists of closely resembling stacking patterns between the two case studies (Figs 7, 12
534 and 15). In both cases, the stacking pattern comprises a lower, fining-upward unit comprising higher-
535 frequency, coarsening-upward facies suites and subordinate glacial surfaces, interpreted as ice-
536 contact glaciomarine deposits which are overlain by a coarsening-upward deltaic system. The lower
537 glaciomarine and upper deltaic wedges have similar thicknesses, each in tens of metres. Finally, the

facies dislocation separating the two wedges in the Ordovician case firmly echoes the GTS identified in the Quaternary example. Thus, having in mind these manifest similarities, the glacial record encompassing the middle unit of the end-Ordovician succession is interpreted as a single and complete deglacial sequence including several backstepping glaciomarine depocenters and an overlying offlapping glaciofluvial delta system that essentially prograded in a context of a RSL fall forced by a glacio-isostatic adjustement. Such an analogy implies that the main part of the end-Ordovician glacial record only relates to a very short-term time interval most likely < 10.000 years. Relative to this depositional duration, the resulting depositional thicknesses, locally in excess of 100 m, are outstanding and at odds with those of usual, non-glacial, shelfal sediment bodies that would have been deposited in a similar timespan. Here, the preserved thickness of the deltaic wedge was essentially controlled by the antecedent glacial erosion depth minus the thickness of the glaciomarine wedge. Assuming a duration of the GIA comparable to that of the Quaternary case studies, average accumulation rates can be inferred for the end-Ordovician to *ca.* 5 $mm.yr^{-1}$ —50 m/10 ka, to be compared with preglacial rates, *ca.* 50 m/ Myr (Loi *et al.* 2010)— evidencing a very active meltwater-derived clastic supply.

Differences between the Quaternary and Ordovician case studies

Differences exist, however, between the Québec North Shore and Anti-Atlas case studies, which call for clarification (Fig. 15). One of the most obvious arises when considering the Ordovician deltaic progradation that may be viewed on the basis of the figure 12 as an extensive feature at the scale of one hundred of kilometres, which departs from spatially restricted (<100-500 km^2) Quaternary deltaic systems emplaced at the mouth of inherited structural valleys (Normandeau *et al*. 2017; Dietrich *et al*. 2017b). One possible explanation would be a longer-term connection of the forced-regressive delta systems to the land-based, retreating ice margins (Fig.15). In the Ordovician epicratonic platform setting, drainage basins are thought to have been much more extensive than the ones of the Québec hinterland, which are comparatively much smaller (<500 km). Therefore, in the North Gondwana configuration, meltwater flows and sediment supply are expected to have been maintained for a greater amount of time, favouring sustained, long-distance progradation in glacio-isostatically-forced regressive deltaic complexes.

A second important difference is the absence in the Ordovician analogue of deep fluvial incision and of sediments related to paraglacial, shallow-marine forced-regressive reworking processes (Fig. 15). If, clearly, forced-regressive shallow-marine deposits may have been superimposed and erased by the succeeding TRS marking the base of the upper transgressive unit, the absence of deeply-incised paraglacial valleys, which would have been expected to accommodate subsequent

transgressive valley fill successions, is questionable. The occurrence of end-Ordovician transgressive deposits truncating and superimposing the overall deglacial sequence suggests a scenario within which the late deglacial eustatic RSL rise had finally overtaken the glacio-isostatically-driven RSL fall. Such a sea-level evolution characterizing the eustatically-dominated zone (Fig. 2) may have occurred in the Anti-Atlas area, relatively close to the end-Ordovician maximum ice margins (Le Heron *et al.* 2007). In this case, an alternative submodern analogue regarding the delta development would be the Gulf of Maine or the offshore of Newfoundland, where currently submerged 'regressive deltas' characterize the post-LGM deglacial record (Figs 2, 9 and 15; Shaw *et al.* 2008; Hein *et al.* 2014 and references therein). Again, and in contrast with Atlantic Canada, which has relatively restricted drainage basins, a longer connection of the deltaic systems to the land-based retreating ice margins is envisioned for the Anti-Atlas case study. Such a setting may have (i) maintained high rate of sediment supply until cessation of the GIA, (ii) favoured the building of larger delta systems, and (iii) potentially allowed the accretion of late glaciofluvial delta built under rising RSL conditions, as also indicated by the consequent thickness of delta plain (Figs 12 and 15). Such a scenario is thought to have occurred as soon as the rates of glacio-isostatic uplift were overtaken by those of the global postglacial transgression that potentially occurred a few thousands of years after deglaciation.

Thirdly, the two case studies typify distinct basinal contexts showing different preservation potentials. Preservation potential of the Québec succession is poor, as in this particular setting where the deglacial sequence directly lies on the crystalline bedrock, subsidence is minimal, if any (Dietrich et al., 2017a). A depositional setting shifted towards positions closer to the maximum ice fronts would have arguably favoured preservation potential owing to postglacial flooding (Fig. 2). In contrast, the Moroccan record is part of a thick Palaeozoic sediment pile implying a basin with active subsidence. However, at time scales under consideration —namely thousands to tens of thousands of years, see above—, the control of subsidence on internal stratigraphic patterns is expected to have been ineffective (see also Girard *et al.* 2015). Bearing this in mind, the preservation potential of shallow and proximal deglacial sequences is likely controlled in Morocco by the depth of the initially glacially-eroded trough and, along the Québec North Shore, by the physiography of the submerged shallow shelf off a basement escarpment. In both cases, accommodation space was essentially inherited, initially present by the time of deglaciation onset, though progressively reduced by ongoing RSL fall (see discussion in Normandeau *et al.* 2017). In the Moroccan example, the RSL evolution characterized by a fall 'immediately' followed by a rise, arguably had an influence on the preservation of the deglacial succession.

Subsidence patterns, imposed by tectonics, and at rates one to three orders lower than that of glacially-impacted RSL, only had the potential to control the stacking pattern of successive glacial-

deglacial cycles. It is suspected that such deglacial sequence may characterize only late to final deglacial episodes. Indeed, the post LGM deglacial sequence along the Québec North Shore is almost the only Quaternary depositional wedge preserved above bedrock. Its preservation on the shelf will be only acquired in case of rapid transgression tied to a potential Antarctic melting (ultimate deglaciation), as any next glacial erosion episode will most probably erase most of this post-LGM record —except in deep structural valleys (Lajeunesse, 2014). In the Moroccan example, the deglacial sequence constitutes the main part of the end-Ordovician glacial record, beneath a transgressive sandstone sheet reflecting the ensuing upper Ordovician to lower Silurian transgression, developed on a million years time scale as shown by biostratigraphy (graptolites). Then, in stratigraphic setting where successive glacial-deglacial depositional cycles were superimposed to each other, the last event is the most susceptible to include a deglacial sequence similar to the one documented here. Distinct shallow deglacial sequences may, however, be preserved in a glaciation record where glacial-deglacial depositional cycles have been essentially laterally juxtaposed owing to repetitive deep glacial surfaces of erosion (Ghienne *et al.* 2007a).

The deglacial succession in a sequence stratigraphic framework

In order to facilitate intra- to extrabasinal correlations, deglacial sequences must be considered through the prism of sequence stratigraphy. Sequence stratigraphic schemes have been recently proposed to account for specifics of the glacial setting (*e.g.,* Zecchin *et al.* 2015). Below we address our deglacial sequence and related within-trend Glaciofluvial Transition Surface (GTS) and Paraglacial Transition Surface (PTS) to system tracts and bounding surfaces of the literature.

Extrapolation of the conventional sequence stratigraphic concepts to the Quaternary and Ordovician deglacial successions would easily ascribe the backstepping glaciomarine wedge to a TST. Following Zecchin *et al.* (2015), no highstand system tract would be recognized and the directly overlying deltaic wedge ascribed to a FSST. In this case, the surface bounding the two system tracts is referred to as a MFS, coinciding with a basal surface of forced-regression (Fig. 7d). In Hansen (2004) and Corner (2006), a (deglacial) highstand system tract (DHST) intervenes between the TST and the FSST (Fig. 7d). As positioned at the local onset of glaciofluvial deltaic deposition, our GTS logically echoes, in terms of facies suites, the Maximum Flooding Surface of Hansen (2004), Corner (2006) and Zecchin *et al.* (2015). However, the GTS significance would be best understood as a stratigraphic surface that has no equivalent in a conventional sequence stratigraphic scheme. It indeed marks the onset of a predominant control of RSL on depositional architectures (Fig. 6) after an initial period during which retrogradation of the successive depocentres was virtually only controlled by the pattern of retreating marine-based ice fronts and their related subaqueous grounding lines positions. Also, our GTS is distinct from the Iceberg-rafting Termination Surface (ITS) of Powell & Cooper (2002) as in the

639 Québec North Shore case study, ice-rafted debris have also been occasionally found in prodelta and
640 lower delta slope deposit, which in this case most likely refer to sea-ice drifting (Dietrich *et al.* 2017a).
641 Our PTS is the equivalent of the proglacial-postglacial surface of Corner (2006) which relates
642 to the abrupt change from glacial to non-glacial sediment supply. In the proximal reaches of deltaic
643 complexes, this surface is marked by a facies transition representing the shutdown of sediment supply.
644 In distal offshore settings, sedimentary condensation may occur. Linking our PTS with the MRS
645 (Maximum Retreat Surface) of the Powell and Cooper (2002) model is debatable as their Glacial
646 Minimum System Tract (GMiST) lying above the MRS is deposited while glacier remains in the
647 hinterland. Their MRS, as it is represented by the abrupt occurrence of deltaic facies (prodeltaic
648 turbidites) on hemipelagic deposits would rather correspond in the Québec North Shore setting to an
649 autogenic surface younging basinward and which the occurrence would depend on deltaic
650 progradation rates, ice margin retreat, RSL fall rates and shelf width and depth (transition from unit 3
651 to 6 in Normandeau *et al.* 2017). Their MRS would lie below our PTS and above, or in places
652 superimposed to, in the absence of hemipelagic deposits, our GTS (Fig. 7d).
653 Ascribing a transgressive origin to the basal backstepping part implies to consider the marine
654 ice margin as representative of the shoreline —the ice-shoreline of Zecchin *et al.* (2015)— while land
655 was partly to entirely still covered by ice. An increase of submarine accommodation driven by the
656 thinning-retreat of the ice cover can be envisioned during the glaciomarine ice margin recession
657 irrespective of the RSL evolution. However, during the early glacimarine evolution, the location of deep
658 (hundreds of meters) depocenters, thicknesses and stacking patterns of associated subaqueous ice-
659 contact deposits are not governed by any equilibrium between accommodation and sediment supply,
660 but solely by the position and timing of the subaqueous sediment entry points along with the geometry
661 of the ice margin (*e.g.,* Brookfield and Martini, 1999; Powell and Cooper, 2001; Dowdeswell and Fugelli,
662 2012). This point generally corresponds to the ice-sheet grounding line and may be significantly distinct
663 from the 'ice-shoreline' which does not discharge any sediment flux especially in case of the presence
664 of an ice shelf. Only close to the marine to continental turnover, the position of the sea level can
665 physically limit accommodation space, forcing the transition from a subaqueous ice-contact fan to an
666 ice-contact delta (Powell, 1990; Lønne, 1995; Lønne *et al.* 2001; Dietrich *et al.* 2017a; Lajeunesse *et al.*
667 this volume). The question which therefore arises is whether or not the application of a conventional
668 sequence stratigraphic nomenclature to deglacial depositional systems without a true shoreline is
669 appropriate. We propose, following Powell and Cooper (2002), that the deglacial sediment body
670 bounded at its base by a glacial surface of erosion and which would include a lower backstepping
671 glaciomarine and an upper forced-regressive deltaic and coastal systems might be better accounted
672 for by using a dedicated deglacial nomenclature. Accordingly, we put forward a Glacial Retreat System
673 Tract (GRST) bounded at its base by a Glacial Surface of Erosion (GSE) and at its top by a Transgressive

674 Ravinement Surface (TRS; Figs 7 and 15); GTS and PTS constituting within-trend stratigraphic surfaces.
675 The GRST can thus be further subdivided into early (between the GSE and the GTS), middle (GTS to
676 PTS) and late (PTS to TRS) entities (Figs 7 and 15). The overlying transgressive system tract *sensu stricto*
677 would be emplaced if, during later stages of deglaciation, sediment supply —meltwater-derived or
678 not— is not able to compete with the glacio-eustatically driven RSL rise (Fig. 15). This 'true' TST
679 genetically linked with a RSL rise would correspond to an early interglacial interval. In that way, a
680 glacial-deglacial sequence bounded below and above, and far from the ice front, by maximum flooding
681 surfaces of the genetic stratigraphy —or more commonly by glacial surfaces of erosion in ice-proximal
682 areas, see Zecchin *et al.* (2015)— will include a single TST, if any; the latter lying atop a GRST in formerly
683 glacio-isostatically depressed areas. Other system tracts of the glacial-deglacial sequence will be
684 normally found in more ice distal situations, where less glacial erosion and a glacio-isostatic
685 adjustement of lesser amplitude occurred (Powell and Cooper, 2001; Le Heron and Busfield, 2016).

686 Finally, we would like to stress that one of the main issues in deciphering a palaeoglacial
687 development from the rock record is probably to properly recognize the nature of the delta system
688 overlying a glaciomarine wedge, with neither the help of high-resolution ages nor the possibility of a
689 fair and absolute correlation datum. Based on our study, comparing a post-LGM to a deep-time
690 records, we thus propose that thick (tens of metres) successions, comprising a lower glaciomarine
691 wedge and an upper deltaic system can confidently be interpreted as 1) a single deglacial sequence
692 that 2) was emplaced in a few thousands of years, 3) under condition of RSL fall forced by the glacio-
693 isostatic adjustement. The possibility of thick but short-term forced-regressive deposits tied to glacio-
694 isostatic processes has been largely underestimated in geological archives as related deltaic deposits,
695 ranging from turbidite systems to tidally-influenced delta plains lack any facies specifics. Further,
696 conventional attributes of forced regression such fluvial incisions can even be absent in some
697 conditions in spite of outstandingly high rates of RSL fall. Resulting depositional thicknesses favour *a-*
698 *priori a* postglacial highstand interpretation though glacio-eustatically-driven FSST tied to a succeeding
699 glacial cycle could also be proposed. The identification of thick deglacial successions emplaced during
700 a glacio-isostatic adjustement is then of paramount importance when estimating the relative duration
701 of successive units, for instance in subsidence analysis or in the study of speciation processes in
702 postglacial recovery faunas (Ghienne *et al*. 2014). If a >100 meter-thick shallowing-upward succession
703 may classically represent a 1-3 Myr time interval in a preglacial context (see Loi *et al.* 2010 for the
704 Moroccan case study), it can be considered as deposited sub-instantaneously (<10 ka) at the geological
705 time scale in a immediately postglacial context. There is a clear distortion of stratigraphic tempos in
706 glaciation-related depositional sequences, within which the time "is going faster" throughout the
707 stratal record.

Conclusions

Based on well-constrained Quaternary analogues, generic characters of a deglacial sequence have been illustrated. Albeit the sedimentary succession representing the deglacial sequence might appear as a conventional transgressive-regressive cycle, it has been emplaced under conditions of high rates (1-10 cm.year^{-1}) of falling RSL forced by the glacio-isostatic adjustement. The deglacial sequence is formed by a thick sedimentary succession reaching 100 m, which is ascribed to a full Glacial Retreat System Tract (GRST) that represents a very short time interval (thousands of years). The architecture of the backstepping glaciomarine depocenters, constituting an early GRST, was mainly controlled by the retreat pattern of the marine-based ice margin including successive ice-front stillstands. The middle GRST is separated from the underlying glaciomarine wedge by the Glaciofluvial Transition Surface (GTS). It relates to seemingly non-glacial turbiditic, deltaic and fluvial facies suites, which were however supplied in glaciogenic material from a retreating ice margin. The unusual thickness of sediment deposited in a context of forced regression and representing a short time interval was achieved by the large amount of sediments supplied by the retreating ice margin as long as it remained connected with the drainage basin. Finally, paraglacial coastal deposits, i.e., sediments decoupled from any glacial influence, are the main component of the late GRST.

There was then an attempt to export specifics of the Québec North Shore deglacial sequence in the Ordovician world for which accurate temporal constraints are intrinsically lacking. In this deep-time setting, comparable facies suites, stratigraphic stacking patterns and intervening stratigraphic surfaces —mainly, a backstepping glaciomarine depocenter below, separated from an above delta succession by a GTS— have been observed, strongly suggesting analogies in the timing and sequence of events of the deglaciation. Then, the > 100 m Ordovician GRST might only represent a few thousand to tens of thousands of years enduring RSL fall forced by the glacio-isostatic adjustement. Such a sub-instantaneous depositional event might significantly change the interpretation of the Late Ordovician glacial record having in mind that this sedimentary sequence represents a significant proportion (>75%) of the thickness of the entire Late Ordovician glacially-related succession that is thought to represent *ca.* 2 Ma. This study thus challenges interpretation of ancient deglacial successions in which deposits that do not appear as glaciogenics at first glance such as deltaic, turbiditic or fluvial but lying on 'true' glaciogenic successions such as grounding-zone wedge accumulations or outwash fans might encompass a very restricted period of time recording the final demise of the ice sheet.

The stacking pattern of a deglacial sedimentary succession and the intervening major stratigraphic surfaces depend at the first order upon the ice-margin retreat patterns and the extent of the drainage basin in the deglaciating hinterland, the combination of both controlling the amount of sediment supplied to the coast. The inherited basin physiography (presence/absence of a shallow

shelf, inherited glacial troughs, coastal escarpment etc.) also has a major influence on the thickness and stratal architecture of the Glacial Retreat System Tract. Intervening stratigraphic surfaces (GTS and PTS) are mainly uncoupled to any change in RSL variations. The effect of RSL change on the deposition of a deglacial sequence, which is very limited during the initial deposition of early glaciomarine suites (early GRST) becomes progressively more important from the emergence of the sedimentary system and during its paraglacial evolution (middle and late GRST).

Acknowledgements

The authors are grateful to Dan Le Heron for his invitation to submit a paper as well as Marie Busfield for her editorial work. Authors are thankful to Philip Hirst and Jörg Lang whose thorough reviews, corrections and comments were insightful and greatly contributed to the improvement of the manuscript. Field campaigns and datings have been funded by action SYSTER and the ARTEMIS program (LMC14) of INSU-CNRS. This work is a contribution to the 'SeqStrat-Ice' ANR project 12-BS06-14.

References

Bernatchez, P. (2003) *Evolution littorale Holocène et actuelle des complexes deltaïques de Betsiamites et de Manicouagan - Outardes : synthèse, processus, causes et perspectives*, Université Laval, Québec.

Bernatchez, P. and Dubois, J.-M.M. (2004) Bilan des connaissances de la dynamique de l'érosion des côtes du Québec maritime laurentien. *Géographie physique et Quaternaire*, **58,** 45-71.

Billy, J., Robin, N., Hein, C.J., Certain, R. and FitzGerald, D.M. (2014) Internal architecture of mixed sand-and-gravel beach ridges: Miquelon-Langlade Barrier, NW Atlantic. *Marine Geology*, **357,** 53-71.

Blum, M., Martin, J., Milliken, K. and Garvin, M. (2013) Paleovalley systems: Insights from Quaternary analogs and experiments. *Earth-Science Reviews*, **116,** 128-169.

Boote, D.R.D., Clark-Lowes, D.D. and Traut M.W. (1998) Paleozoic petroleum systems of North Africa. In: *Petroleum Geology of North Africa* (Eds D.S. Macgregor, R.T.J. Moody and D.D. Clark-Lowes), *Geol. Soc. London Spec. Publ.*, **132**, 7–68.

Boulton, G.S. (1990) Sedimentary and sea level changes during glacial cycles and their control on glacimarine facies architecture. In: *Glacimarine Environments: Processes and sediments* (Eds J.A. Dowdeswell and J.D. Scourse), **53**, 15-52. Geological Society Special Publication, London.

Bourahrouh, A., Paris, F. and Elaouad-Debbaj, Z. (2004) Biostratigraphy, biodiversity and palaeoenvironments of the chitinozoans and associated palynomorphs from the Upper Ordovician of the Central Anti-Atlas, Morocco. *Review of Palaeobotany and Palynology*, **130,** 17-40.

Boyer-Villemaire, U., St-Onge, G., Bernatchez, P., Lajeunesse, P. and Labrie, J. (2013) High-resolution multiproxy records of sedimentological changes induced by dams in the Sept-Îles area (Gulf of St. Lawrence, Canada). *Marine Geology*, **338,** 17-29.

Brinkerhoff, D., truffer, M. and Aschwanden, A. (2017) Sediment transport drives tidewater glacier periodicity. *Nature Communications*, **8**.

Brookfield, M.E. and Martini, I.P. (1999) Facies architecture and sequence stratigraphy in glacially influenced basins: basic problems and water-level/glacier input-point controls (with an example from the Quaternary of Ontario, Canada). *Sedimentary Geology*, **123,** 183-19.

Burkhard, M., Caritg, S., Helg, U., Robert-Charrue, C. and Soulaimani, A. (2006) Tectonics of the Anti-Atlas of Morocco. *Comptes Rendus Geoscience*, **338,** 11-24.

Church, M. (1972) Baffin Island sandurs: a study of Arctic fluvial processes. *Geological Survey of Canada*, **Bulletin 216,** 208 pp.

Church, M. (2006) Bed material transport and the morphology of alluvial river channels. *Annual Reviews of Earth Planetary Sciences*, **34,** 325-354.

Clerc, S., Buoncristiani, J.-F., Guiraud, M., Vennin, E., Desaubliaux, G. and Portier, E. (2013) Subglacial to proglacial depositional environments in an Ordovician glacial tunnel valley, Alnif, Morocco. *Palaeogeography, Palaeoclimatology, Palaeoecology*, **370,** 127-144.

Corner, G.D. (2006) A transgressive-regressive model of fjord-valley fill: stratigraphy, facies and depositional controls. In: *Incised-valley Systems in Time and Space.* SEPM Special Publication (Eds R.W. Dalrymple, D. Leckie and R. Tilman), **85**, 161-178.

Creveling, J.R., Bergmann, K.D. and Grotzinger, J.P. (2016) Cap carbonate platform facies model, Noonday Formation, SE California. *Geological Society of America Bulletin*, **128,** 1249-1269.

Creveling, J.R. and Mitrovica, J.X. (2014) The sea-level fingerprint of a Snowball Earth deglaciation. *Earth and Planetary Science Letters*, **399,** 74-85.

Denis, M., Buoncristiani, J.-F. and Guiraud, M. (2009) Fluid-pressure controlled soft-bed deformation sequence beneath the surging Breiðamerkurjökull (Iceland, Little Ice Age). *Sedimentary Geology*, **221,** 71-86.

Deschamps, R., Eschard, R. and Roussé, S. (2013) Architecture of Late Ordovician tunnel valleys in the Tassili N'Ajjer area (Algeria). *Sedimentary Geology*, **289**, 124-147.

Destombes, J. (1968) Sur la présence d'une discordance générale de ravinement d'âge Ashgill supérieur dans l'Ordovicien terminal de l'Anti-Atlas (Maroc). *Comptes Rendus de l'Academie de Sciences*, **267**, 565-567.

Destombes, J. (1985) Notice explicative de la carte géologique du Maroc au 200.000ème "Todhra-Maïder"(Anti-Atlas oriental). Cambrien moyen, Ordovicien, base du Silurien. *Rapport du Service de la Carte géologique du Maroc*.

Deynoux, M. and Ghienne, J.-F. (2004) Late Ordovician glacial pavements revisited: a reappraisal of the origin of striated surfaces. *Terra Nova*, **16,** 95-101.

Dietrich, P., Ghienne, J.-F., Normandeau, A. and Lajeunesse, P. (2016a) Upslope-Migrating Bedforms In A Proglacial Sandur Delta: Cyclic Steps From River-Derived Underflows? *Journal of Sedimentary Research*, **86,** 113-123.

Dietrich, P., Ghienne, J.F., Darnault, R., Deschamps, R., Berrada, I., El Houicha, M., Giannone, M., Maillot, B., Razin, P. and Schmitz, J. (2016b) Glaciotectonic complexes in the central Anti-Atlas (Morocco): Implications regarding the end-Ordovician ice-margin dynamics. In: *35th International Geological Congress*, Cape Town, South Africa. http://www.americangeosciences.org/sites/default/files/igc/771.pdf

Dietrich, P., Ghienne, J.-F., Schuster, M., Lajeunesse, P., Nutz, A., Deschamps, R., Roquin, C. and Duringer, P. (2017a) From outwash to to coastal systems in the Portneuf-Forestville

826 deltaic complex (Québec North Shore): Anatomy of a forced regressive deglacial sequence.
827 *Sedimentology*, **64**, 1044-1078.

828 **Dietrich, P. Ghienne, J.-F., Normandeau, A. and Lajeunesse, P.** (2017b) Reconstructing ice-
829 margin retreat using delta morphostratigraphy. *Scientific Reports*, **16936**, doi:
830 10.1038/s41598-017-16763-x

831 **Dionne, J.-C. and Occhietti, S.** (1996) Aperçu du Quaternaire à l'embouchure du Saguenay,
832 Québec. *Géographie physique et Quaternaire*, **50,** 5-34.

833 **Dowdeswell, J.A. and Fugelli, E.M.G.** (2012) The seismic architecture and geometry of
834 grounding-zone wedges formed at the marine margins of past ice sheets. *Geological Society*
835 *of America Bulletin,* **124**, 1750-1761.

836 **Drapeau, G.** (1992) Dynamique sédimentaire des littoraux de l'estuaire du Saint-Laurent.
837 *Géographie physique et Quaternaire*, **46,** 233.

838 **Dredge, L.A.** (1983) Surficial geology of the Sept-Iles area, Quebec North Shore. *Geological*
839 *Survey of Canada Memoir 408***,** 40.

840 **Duchesne, M.J., Pinet, N., Bédard, K., St-Onge, G., Lajeunesse, P., Campbell, D.C. and Bolduc,**
841 **A.** (2010) Role of the bedrock topography in the Quaternary filling of a giant estuarine basin:
842 the Lower St. Lawrence Estuary, Eastern Canada. *Basin Research*.

843 **Dunbar, G.B., Naish, T., Barrett, P.J., Fielding, C.R. and Powell, R.** (2008) Constraining the
844 amplitude of late Oligocene bathymetric changes in Western Ross Sea during orbitally-
845 induced oscillations in the East Antarctic Ice Sheet:(1) Implications for glacimarine sequence
846 stratigraphic models. *Palaeogeography, Palaeoclimatology, Palaeoecology*, **260,** 50-65.

847 **Dyke, A.S. and Peltier, W.R.** (2000) Forms, response times and variability of relative sea-level
848 curves, glaciated North America. *Geomorphology*, **32,** 315 - 333.

849 **Eilertsen, R.S., Corner, G.D., Assheim, O. and Hansen, L.** (2011) Facies characteristics and
850 architecture related to palaeodepth of Holocene fjord-delta sediments. *Sedimentology*, **58,**
851 1784-1809.

852 **Evans, D.J.A., Phillips, E.R., Hiemstra, J.F. and Auton, C.A.** (2006) Subglacial till: Formation,
853 sedimentary characteristics and classification. *Earth-Science Reviews*, **78,** 115-176.

854 **Eyles, N. and Eyles, C., H.** (1992) Glacial Depositional Systems. In: *Facies, Models, Respons to*
855 *sea-level change* (Eds R.G. Walker and N.P. James), 73-100. Geological Association of Canada,
856 Toronto.

857 **Forbes, D.L. and Syvitski, J.P.** (1994) Paraglacial coasts. In: *Coastal Evolution: Late Quaternary*
858 *Shoreline Morphodynamics* (Eds R.W.G. Carter and C.D. Woodroffe), 373-424. Cambridge
859 University Press, Cambridge.

860 **Ghienne, J.-F.** (2003) Late Ordovician sedimentary environments, glacial cyclces, and post-
861 glacial transgression in the Taoudeni Basin, West Africa, *Palaeogeography, Palaeoclimatology,*
862 *Palaeoecology*, **189**, 117-145.

863 **Ghienne, J.-F., Girard, F., Moreau, J. and Rubino, J.-L.** (2010) Late Ordovician climbing-dune
864 cross-stratification: a signature of outburst floods in proglacial outwash environments?
865 *Sedimentology*, **57**, 1175-1198.

866 **Ghienne, J.-F., Le Heron, D.P., Moreau, J., Denis, M. and Deynoux, M.** (2007) The Late
867 Ordovician glacial sedimentary system of the North Gondwana platform. In: *Glacial*
868 *Sedimentary Processes and Products* (Eds Hambrey, M.J., Christoffersen, P., Glasser, N.F. and
869 Hubbard, B.) Special Publication 39 of the International Association of Sedimentologists, 290-
870 319.

871 **Ghienne, J.F., Boumendjel, K., Paris, F., Videt, B., Racheboeuf, P. and Salem, H.A.** (2007b)
872 The Cambrian-Ordovician succession in the Ougarta Range (western Algeria, North Africa) and
873 interference of the Late Ordovician glaciation on the development of the Lower Palaeozoic
874 transgression on northern Gondwana. *Bulletin of Geosciences*, **82**, 183-214.

875 **Ghienne, J. F., Moreau, J., Degermann, L. and Rubino, J. L.** (2013) Lower Palaeozoic
876 unconformities in an intracratonic platform setting: glacial erosion versus tectonics in the
877 eastern Murzuq Basin (southern Libya). *International Journal of Earth Sciences*, **102**, 455-482.

878 **Ghienne, J.F., Desrochers, A., Vandenbroucke, T.R.A., Achab, A., Asselin, E., Dabard, M.P.,**
879 **Farley, C., Loi, A., Paris, F., Wickson, S. and Veizer, J.** (2014) A Cenozoic-style scenario for the
880 end-Ordovician glaciation. *Nature Communication*, **5,** 1-9.

881 **Girard, F., Ghienne, J.-F., Du-Bernard, X. and Rubino, J.-L.** (2015) Sedimentary imprints of
882 former ice-sheet margins: Insights from an end-Ordovician archive (SW Libya). *Earth-Science*
883 *Reviews*.

884 **Hansen, L.** (2004) Deltaic infill of a deglaciated arctic fjord, East Greenland: sedimentary facies
885 and sequence stratigraphy. *Journal of Sedimentary Research*, **74,** 422-437.

886 **Hart, B.S. and Long, B.F.** (1996) Forced regressions and lowstand deltas: Holocene Canadian
887 examples. *Journal of Sedimentary Research*, **66,** 820-829.

888 **Haldorsen, S., Von Bruun, V., Maud, R. and Truter, E.D.** (2001) A Weichselian deglaciation
889 model applied to the Early Permian glaciation in the northeast Karoo Basin, South Africa.
890 *Journal of Quaternary Science,* **16**, 583-593.

891 **Hein, C.J., FitzGerald, D.M., Buynevich, I.V., Van Heteren, S. and Kelley, J.T.** (2014) Evolution
892 of paraglacial coasts in response to changes in fluvial sediment supply. In: *Sedimentary Coastal*
893 *Zones from high to low latitudes: similarities and differences* (Eds. Martini, I.P. and Wanless,
894 H.R.), **388,** 247-280, *Geological Society, London, Special Publications*.

895 **Hein, F.J., Syvitski, J.P.M., Dredge, L.A. and Long, B.F.** (1993) Quaternary sedimentation and
896 marine placers along the North Shore, Gulf of St-Lawrence. *Canadian Journal of Earth Sciences*,
897 **30,** 553 - 574.

898 **Helland-Hansen, W. and Hampson, G.J.** (2009) Trajectory analysis: concepts and applications.
899 *Basin Research*, **21,** 454-483.

900 **Hirst, J.P.P.** (2012) Ordovician proglacial sediments in Algeria: insights into the controls on
901 hydrocarbon reservoirs in the Amenas field, Illizi Basin. In: *Glaciogenic Reservoirs and*
902 *Hydrocarbon Systems* (Eds. Huuse, M., Redfern, J., Le Heron, D.P., Dixon R.J., Moscariello, A.
903 and Craig, J.), **368**, 319-353, Geological Society of London, Special Publication.

Holbrook, J.M. and Bhattacharya, J.P. (2012) Reappraisal of the sequence boundary in time and space: Case and considerations for an SU (subaerial unconformity) that is not a sediment bypass surface, a time barrier, or an unconformity. *Earth-Science Reviews*, **113,** 271-302.

Hunt, D. and Tucker, M.E. (1992) Stranded parasequences and the forced regressive wedge systems tract: deposition during base-level fall. *Sedimentary Geology*, **81,** 1-9.

Josenhans, H. and Lehman, S. (1999) Late glacial stratigraphy and history of the Gulf of St. Lawrence, Canada. *Canadian Journal of Earth Sciences*, **36,** 1327-1344.

Kearey, P., Klepeis, K.A. and Vine, F.J. (2009) *Global Tectonics*. Wiley-Blackwell, Chichester - UK.

Koohzare, A., Vaníček, P. and Santos, M. (2008) Pattern of recent vertical crustal movements in Canada. *Journal of Geodynamics*, **45,** 133-145.

Lajeunesse, P., Locat, J., St. Onge, G. and Labbé, G. (2007) Morphosedimentology of submarine mass-movements and gravity flows offshore Sept-Îles, NW Gulf of St. Lawrence (Québec, Canada). In *Submarine Mass Movements and Their Consequences* (Eds V. Lykousis, D. Sakellariou and J. Locat) (pp. 287-296). Springer Netherlands.

Lajeunesse, P. and St-Onge, G. (2013) Late-Wisconsinan submarine moraines along the north shore of the Estuary and Gulf of St. Lawrence (Eastern Canada). European Geosciences Union (EGU) General Assembly.

Lajeunesse, P. (2014) Buried preglacial fluvial gorges and valleys preserved through Quaternary glaciations beneath the eastern Laurentide Ice Sheet. *Geological Society of America Bulletin*, **126**, 447-458.

Lajeunesse, P. (2016) Late-Wisconsinan grounding-zone wedges, northwestern Gulf of St. Lawrence (eastern Canada). In: *Atlas of submarine glacial landforms* (Eds J.A. Dowdeswell, M. Canals, M. Jakobsson, B.J. Todd, E.K. Dowdeswell and K.A. Hogan), **46**, 227-228. Geological Society, London, Memoirs.

Lajeunesse, P., Dietrich, P. and Ghienne, J.F. (this volume) Late-Wisconsinan grounding zones of the Laurentide Ice Sheet margin off the Québec North Shore (NW Gulf of St. Lawrence). *Geological Society of London, Special Publication.*

Lambeck, K., Purcell, A. and Dutton, A. (2012) The anatomy of interglacial sea levels: The relationship between sea levels and ice volumes during the Last Interglacial. *Earth and Planetary Science Letters*, **315-316,** 4-11.

Leeder, M.R. and Stewart, M.D. (1996) Fluvial incision and sequence stratigraphy: alluvial responses to relative sea-level fall and their detection in the geological record. In: *Sequence stratigraphy in British Geology* (Eds S.P. Hesselbo and D.N. Parlinson), **103**, 25-39. Geological Society Special Publication.

Le Heron, D.P., Sutcliff, O.E., Whittington, R.J. and Craig, J. (2005) The origins of glacially related soft-sediment deformation structures in Upper Ordovician glaciogenic rocks: implications for ice sheet dynamics. *Palaeogeography, Palaeoclimatology, Palaeoecology*, **218**, 75-103.

Le Heron, D.P., Craig, J., Sutcliff, O.E. and Whittington, R. (2006) Glaciogenic reservoir heterogeneity: an example from the Late ordovician of the Murzuq Basin, SW Libya. *Marine and Petroleum Geology*, **23**, 655-677.

Le Heron, D.P., Ghienne, J.F., El Houicha, M., Khoukhi, Y. and Rubino, J.L. (2007) Maximum extent of ice sheets in Morocco during the Late Ordovician glaciation. *Palaeogeography, Palaeoclimatology, Palaeoecology*, **245**, 200-226.

Le Heron, D.P. (2007) Late Ordovician glacial record of the Anti-Atlas, Morocco. *Sedimentary Geology*, **201**, 93-110.

Le Heron, D.P. and Craig, J. (2008) First-order reconstructions of the Late Ordovician Saharan ice sheet. *Journal of the Geological Society,* **165**, 19-29.

Le Heron, D.P. (2012) The Cryogenian record of glaciation and deglaciation in South Australia. *Sedimentary Geology,* **243**, 57-69.

Le Heron, D.P. (2016) The Hirnantian glacial landsystem of the Sahara: a meltwater-dominated system. In: *Atlas of submarine glacial landforms* (Eds J.A. Dowdeswell, M. Canals, M. Jakobsson, B.J. Todd, E.K. Dowdeswell and K.A. Hogan), **46**, 509-516. Geological Society, London, Memoirs.

Le Heron, D.P. and Busfield, M.E. (2016) Pulsed iceberg delivery driven by Sturtian ice sheet dynamics: An example from the Death Valley, California, *Sedimentology*, **63**, 331-349.

Le Heron, D.P., Tofaif, S., Vandyk, T. and Ali, D.O. (2017) A diamictite dichotomy: Glacial conveyor belts and olistostromes in the Neoproterozoic of Death Valley, California, USA. *Geology*, **45**, 31-34.

Loi, A., Ghienne, J.F., Dabard, M.P., Paris, F., Botquelen, A., Christ, N., Elaouad-Debbaj, Z., Gorini, A., Vidal, M., Videt, B. and Destombes, J. (2010) The Late Ordovician glacio-eustatic record from a high-latitude storm-dominated shelf succession: The Bou Ingarf section (Anti-Atlas, Southern Morocco). *Palaeogeography, Palaeoclimatology, Palaeoecology*, **296,** 332-358.

Lønne, I. (1995) Sedimentary facies and depositional architecture of ice-contact glaciomarine systems. *Sedimentary Geology*, **98,** 13-43.

Lønne, I., Nemec, W., Blikra, L.H. and Lauritsen, T. (2001) Sedimentary architecture and dynamic stratigraphy of a marine ice-contact system. *Journal of Sedimentary Research*, **71,** 922 - 943.

Lüning, S., Craig, J., Loydell, D. K., Štorch, P. and Fitches, B. (2000) Lower Silurian hot shales in North Africa and Arabia: regional distribution and depositional model. *Earth-Science Reviews*, **49**, 121-200.

Mottin, T.E., Vesely, F.F., de Lima Rodriguez, M.C.N., Kipper, F. and de Souza, P.A. (2017) The paths and timing of late Paleozoic ice revisited: New stratigraphic and paleo-ice flow interpretations from a glacial succession in the upper Itararé Group (Paraná Basin, Brazil). *Palaeogeography, Palaeoclimatology, Palaeoecology*, **490**, 488-504.

Moreau, J. (2011) The Late Ordovician deglaciation sequence of the SW Murzuq Basin (Libya), *Basin Research*, **23**, 449-477.

Moreau, J. and Ghienne, J.-F. (2016) Cross-shelf trough and ice-stream lineations in the 440 Ma Late Ordovician rocks of northern Africa mapped from high-resolution satellite imagery. In: *Atlas of submarine glacial landforms* (Eds J.A. Dowdeswell, M. Canals, M. Jakobsson, B.J. Todd, E.K. Dowdeswell and K.A. Hogan), **46**, 173-174. Geological Society, London, Memoirs.

Muto, T. and Steel, R.J. (2004) Autogenic response of fluvial deltas to steady sea-level fall: implications from flume-tank experiments. *Geology*, **32**, 401-404.

Normandeau, A., Lajeunesse, P. and St-Onge, G. (2013) Shallow-water longshore drift-fed submarine fan deposition (Moisie River Delta, Eastern Canada). *Geo-Marine Letters*, **33,** 391-403.

Normandeau, A., Lajeunesse, P. and St-Onge, G. (2015) Submarine canyons and channels in the Lower St. lawrence Estuary (eastern Canada): Morphology, classification and recent sediment dynamics. *Geomorphology*, **241**, 1-18.

Normandeau, A., Dietrich, P., Lajeunesse, P., St-Onge, G., Ghienne, J.-F., Duchesne, M. and Francus, P. (2017) Timing and controls on the delivery of coarse sediment to deltas and submarine fans on a formerly glaciated coast and shelf. *Geological Society of America Bulletin.*

Nutz, A., Ghienne, J.-F., Schuster, M., Dietrich, P., Roquin, C., Hay, M.B., Bouchette, F. and Cousineau, P.A. (2015) Forced regressive deposits of a deglaciation sequence: example from the Late Quaternary succession in the Lake Saint-Jean basin (Québec, Canada). *Sedimentology*, **62**, 1573-1610.

Nutz, A., Ghienne, J.F. and Storch, P. (2013) Circular, Cryogenic Structures from the Hirnantian Deglaciation Sequence (Anti-Atlas, Morocco). *Journal of Sedimentary Research*, **83,** 115-131.

Occhietti, S. (2007) The Saint-Narcisse morainic complex and early Younger Dryas events on the southeastern margin of the Laurentide Ice Sheet. *Géographie physique et Quaternaire*, **61,** 89-117.

Occhietti, S., Parent, M., Lajeunesse, P., Robert, F. and Govare, É. (2011) Late Pleistocene–Early Holocene Decay of the Laurentide Ice Sheet in Québec–Labrador. **15,** 601-630.

Patruno, S., Hampson, G.J. and Jackson, C.A.L. (2015) Quantitative characterisation of deltaic and subaqueous clinoforms. *Earth-Science Reviews*, **142,** 79-119.

Pazos, P.J. (2002) The Late Carboniferous Glacial to Postglacial Transition: Facies and Sequence Stratigraphy, Western Paganzo Basin, Argentina. *Gondwana Research*, **5,** 467-487.

Peltier, W.R., Argus, D.F. and Drummond, R. (2015) Space geodesy constrains ice age terminal deglaciation: The global ICE-6G_C (VM5a) model. *Journal of Geophysical Research: Solid Earth*, **120,** 450-487.

Pinet, N., Brake, V. and Duchesne, M. (2016) Partly-filled U-shaped morphology of the Laurentian Channel, St. Lawrence Estuary, Canada. In: *Atlas of submarine glacial landforms* (Eds J.A. Dowdeswell, M. Canals, M. Jakobsson, B.J. Todd, E.K. Dowdeswell and K.A. Hogan), **46**, 163-164. Geological Society, London, Memoirs.

Powell, R.D. (1990) Glacimarine processes at grounding-line fans and their growth to ice-contact deltas. In: *Glacimarine Environments: Processes and Sediments* (Eds J.A. Dowdeswell and Scourse, J.D.), **53**, 53-73, Geological Society Special Publication.

Powell, R.D. and Cooper, J.M. (2002) A glacial sequence stratigraphic model for temperate, glaciated continental shelves. In: *Glacier-influenced sedimentation on High-Latitude Continental Margins* (Eds Dowdeswell, J.A. and O Cofaigh, C.), **203**, 215-244, Geological Society Special Publication.

Prince, G.D. and Burgess, P.M. (2013) Numerical Modeling of Falling-Stage Topset Aggradation: Implications for Distinguishing Between Forced and Unforced Regressions In the Geological Record. *Journal of Sedimentary Research*, **83,** 767-781.

Ravier, E., Buoncristiani, J. F., Menzies, J., Guiraud, M., Clerc, S., and Portier, E. (2015) Does porewater or meltwater control tunnel valley genesis? Case studies from the Hirnantian of Morocco. *Palaeogeography, Palaeoclimatology, Palaeoecology*, **418**, 359-376**.**

Reimer, P.J., Baillie, M.G.L., E., B., Bayliss, A., Beck, J.W., Blackwell, P.G., Bronk Ramsey, C., Buck, C.E., Burr, G.S., Edwards, R.L., Friedrich, M., Grootes, P.M., Guilderson, T.P., Hajdas, I., Heaton, T.J., Hogg, A.G., Hughen, K.A., Kaiser, K.F., Kromer, B., McCormac, F.G., Manning, S.W., Reimer, R.W., Richards, D.A., Southon, J.R., Talamo, S., Turney, C.S.M., van der Plicht, J. and Weyhenmeyer, C.E. (2009) IntCal09 and Marine09 radiocarbon age calibration curves, 0-50,000 years Cal BP. *Radiocarbon*, **51,** 1111-1150.

Sella, G.F., Stein, S., Dixon, T.H., Craymer, M., James, T.S., Mazzotti, S. and Dokka, R.K. (2007) Observation of glacial isostatic adjustment in “stable” North America with GPS. *Geophysical Research Letters*, **34**.

Shaw, J., Gareau, P. and Courtney, R.C. (2002) Palaeogeography of Atlantic Canada 13-0 kyr. *Quaternary Science Reviews*, **21,** 1861-1878.

Shaw, J., Grant, D.R., Guilbault, J.P., Anderson, T.W. and Parrott, D.R. (2008) Submarine and onshore end moraines in southern Newfoundland: implications for the history of late Wisconsinan ice retreat. *Boreas*, **29,** 295-314.

Shaw, J., Piper, D.J.W., Fader, G.B.J., King, E.L., Todd, B.J., Bell, T., Batterson, M.J. and Liverman, D.G.E. (2006) A conceptual model of the deglaciation of Atlantic Canada. *Quaternary Science Reviews*, **25,** 2059-2081.

St-Onge, G., Lajeunesse, P., Duchesne, M. J., and Gagne, H. (2008). Identification and dating of a key Late Pleistocene stratigraphic unit in the St. Lawrence Estuary and Gulf (Eastern Canada). *Quaternary Science Reviews*, **27**, 2390-2400.

Stocchi, P., Escutia, C., Houben, A.J.P., Vermeersen, B.L.A., Bijl, P.K., Brinkhuis, H., DeConto, R., Galeotti, S., Passchier, S., Pollard, D. and scientists, I.E. (2013) Relative sea-level rise around East Antarctica during Oligocene glaciation. *Nature Geoscience*, **6,** 380-384.

Stokes, C.R., Tarasov, L., Blomdin, R., Cronin, T.M., Fisher, T.G., Gyllencreutz, R., Hättestrand, C., Heyman, J., Hindmarsh, R.C.A., Hughes, A.L.C., Jakobsson, M., Kirchner, N., Livingstone, S.J., Margold, M., Murton, J.B., Noormets, R., Peltier, W.R., Peteet, D.M., Piper, D.J.W., Preusser, F., Renssen, H., Roberts, D.H., Roche, D.M., Saint-Ange, F., Stroeven, A.P. and Teller, J.T. (2015) On the reconstruction of palaeo-ice sheets: Recent advances and future challenges. *Quaternary Science Reviews*, **125,** 15-49.

Storms, J.E.A., de Winter, I.L., Overeem, I., Drijkoningen, G.G. and Lykke-Andersen, H. (2012) The Holocene sedimentary history of the Kangerlussuaq Fjord-valley fill, West Greenland. *Quaternary Science Reviews*, **35,** 29-50.

Strong, N. and Paola, C. (2008) Valleys That Never Were: Time Surfaces Versus Stratigraphic Surfaces. *Journal of Sedimentary Research*, **78,** 579-593.

Sutcliffe, O.E., dowdeswell, J.A., Whittington, R.J., Theron, J.N. and Craig, J. (2000) Calibrating the Late Ordovician glaciation and mass extinction by the eccentricity cycles of Earth's orbit. *Geology*, **28,** 967 - 970.

Swenson, J.B. and Muto, T. (2007) Response of coastal plain rivers to falling relative sea-level: allogenic controls on the aggradational phase. *Sedimentology*, **54,** 207-221.

Swenson, J.B., Paola, C., Pratson, L., Voller, V.R. and Murray, A.B. (2005) Fluvial and marine controls on combined subaerial and subaqueous delta progradation: Morphodynamic modelling of compound-clinoform development. *Journal of Geophysical Research*, **110,** 1-16.

Syvitski, J.P.M. (1989) On the deposition of sediment within glacier-influenced fjords: oceanographic controls. *Marine Geology*, **85,** 301-329.

Syvitski, J.P.M. and Praeg, D.B. (1989) Quaternary Sedimentation in the St. Lawrence Estuary and Adjoining Areas, Eastern Canada: An Overview Based on High-Resolution Seismo-Stratigraphy. *Géographie physique et Quaternaire*, **43,** 291.

Talling, P.J., Masson, D.G., Sumner, E.J. and Malgesini, G. (2012) Subaqueous sediment density flows: Depositional processes and deposit types. *Sedimentology*, **59,** 1937-2003.

Tamisiea, M.E. and Mitrovica, J.X. (2011) The moving boundaries of sea level change: Understanding the origins of geographic variability. *Oceanography*, **24,** 24-39.

Tarasov, L., Dyke, A.S., Neal, R.M. and Peltier, W.R. (2012) A data-calibrated distribution of deglacial chronologies for the North American ice complex from glaciological modeling. *Earth and Planetary Science Letters*, **315-316,** 30-40.

Watts, A.B. (2009) *Crust and lithosphere dynamics*, Oxford, 610 pp.

Willefert, S. (1988) The Ordovician-Silurian boundary in Mauritania. In: *A global analysis of the Ordovician-Silurian boundary. Bulletin of the British Museum (Natural History)* (Eds L.R.M. Cocks and R.B. Rickards), **43**, 177-182.

Woodworth, P.L., Gehrels, W.R. and Nerem, R.S. (2011) Nineteeth and twentieth century changes in sea level, *Oceanography*, **24**, 80-93.

Zecchin, M. (2007) The architectural variability of small-scale cycles in shelf and ramp clastic systems: The controlling factors. *Earth-Science Reviews*, **84,** 21-55.

Zecchin, M., Catuneanu, O. and Rebesco, M. (2015) High-resolution sequence stratigraphy of clastic shelves IV: high-latitude settings. *Marine and Petroleum Geology*.

Figure captions

Fig. 1. Physiography of the Québec North Shore (St. Lawrence Estuary and Gulf). Black lines represent successive positions of the post-LGM retreating LIS margin (from Occhietti *et al.* 2011). The blue dashed line marks the marine limit, i.e., the maximal extent of the postglacial Goldthwait Sea. The Sept-Îles deltaic complex described in the text is localized by the orange star.

Fig. 2. Pattern of relative sea level change in space and time produced by concurrent glacio-isostatic adjustement and glacio-eustatic rise and schematic associated sedimentary successions (not to scale) in Eastern Canada. Curve 1 (Gulf of Maine, Hein *et al.* 2014) represents the eustatically-dominated zone where an early RSL fall forced by the glacio-isostatic adjustement precedes a RSL rise forced by glacio-eustatic processes. The resulting, submerged, stratigraphic succession consists of a forced regressive, shallowing-upward glaciofluvial delta system underlain by subaqueous ice-contact deposits and overlain by a transgressive sand and mud package (see Fig. 9c). Curve 2 (Québec North Shore, Dietrich *et al.* 2017a) represents a continuous RSL fall forced by the glacio-isostatic adjustement (glacio-isostatically dominated zone). The associated sedimentary succession which the present contribution focuses on lies above the modern sea level and consists of a forced-regressive, shallowing-upward glaciofluvial delta system underlain by subaqueous ice-contact deposits. The dotted curve corresponds to the global, i.e., glacio-eustatic, sea level rise (Peltier *et al.* 2015).

Fig. 3. Bathymetry (multibeam) and topography (LiDAR) of the Sept-Îles deltaic complex (Fig. 1 for location). The black bold line represents the trace of the synoptic transect of figure 4. Inset map in the lower right corner represents the drainage basin of the Moisie River including positions of the retreating LIS margin (from Occhietti *et al.* 2011). See Lajeunesse *et al*. (this volume) for details about bathymetric data.

Fig. 4. Synoptic transects of deltaic complexes. (**a**) the Sept-Îles deltaic complex (see location in Fig. 3). Radiocarbon dates (calibration according to Reimer *et al.* 2009) are either original (in black) or derived from the literature (grey). (**b**) Outline of the Portneuf deltaic complex at the same scale as (a) (simplified from Dietrich *et al.* 2017a).

Fig. 5. Depositional facies and architecture of the Sept-Îles glaciofluvial deltaic complex. (**a**) Offlapping geometries in the lower deltaic lobe comprising gently-sloped lower delta slope deposits, steeply-dipping clinothems of the upper delta slope and, at top, erosion-based delta front/ delta plain deposits. (**b**) Lower delta slope deposits showing highly contorted beds, either slump or large-scale load structures. Shovel (1 m) for scale. (**c**) Planar and trough cross-stratified gravelly sand of the delta plain.

(**d**) Subaqueous ice-contact fan deposits, including boulder-sized lonestones overlain by a till layer (boulders on top are not in place).

Fig. 6. The three-staged development of the Sept-Îles deltaic complex from 12.5 to 3.5 cal ka BP: retreat of a marine ice margin and emplacement of backstepping grounding zone wedges, glaciofluvial delta deposition and paraglacial evolution. The successive depocenter trajectory (lower cartoon) shows a large loop (see text for details). The inset represents the RSL fall history in the study area compiled from stratigraphic, sedimentological and radiocarbon studies.

Fig. 7. Interpretation of the Sept-Îles deglacial sequence (**a**) Synthetic log, including a lower fining-upward and an upper coarsening-upward sets. Key to grain size: Sh: shales; Si: siltstones; fgs: fine-grained sandstones; Cgs: coarse-grained sandstones; Cs: conglomeratic sandstones. (**b**) Interpretation in terms of sedimentary processes and ice-margin evolution. (**c**) Apparent system tracts in a conventional, i.e., non-glacial, sequence stratigraphic model and true RSL trend. (**d**) Current and previous conceptual models and nomenclature proposed for interpretation of comparable deglacial sequence; LGM: Last Glacial Maximum; BSFR: Basal Surface of Forced Regression; DST: Deglacial System Tract; FSST: Falling-Stage System Tract; HST: Highstand System Tract; MFS: Maximum Flooding Surface; SU: Subaerial Unconformity; TRS: Transgressive Ravinement Surface; TST: Transgressive System Tract.

Fig. 8. Stratigraphic variability of deglacial sequence illustrated in this contribution and relationships with stratigraphic surfaces depending on the position of the studied succession regarding depocenters. GSE: Glacial Surface of Erosion; GTS: Glaciofluvial Transition Surface; PTS: Paraglacial Transition Surface.

Fig. 9. Synthetic transects of three Quaternary deglacial sequence of eastern Canada illustrating the stratigraphic architecture, bounding surfaces and depositional environments. (**a**) The Portneuf deltaic complex (from Dietrich *et al.* 2017a) as understood from onshore exposure. (**b**) The offshore-onshore transect of the Sept-Îles deltaic complex (see Figs 4 and 6 for details). (**c**) Architecture of the deglacial sequence in the Gulf of Maine showing a Transgressive Ravinement Surface (TRS) and overlying transgressive deposits (modified from Hein *et al.* 2014). (a) and (b) : curve 1 in Fig. 2; (c) curve 2. Note that vertical and horizontal scales are different for each transect.

Fig. 10. NW Africa geological setting. (**a**) Reconstruction of the end-Ordovician ice sheet at its maximum extent. (**b**) Simplified geological map of Morocco with location of the study area (black box). (**c**) Tentative reconstruction of the local palaeoglacial setting on the basis on depositional thicknesses (numbers in white) and ice-flow indications (striae, grooves, glacial lineations: couplets of parallel black

lines). They are compatible with a large glacial trough, the axis of which was more or less parallel to the depositional dip of the underlying clinoforms (Fig. 11). An eastward ice flow is inferred from a lodged pebble (western white arrow) and a glaciotectonic fold-and-thrust belt (eastern white arrow). The Tagounite Trough (dashed line) is an Upper Ordovician depocenter, which may have re-oriented regional-scale ice flows.

Fig. 11. Cross profile showing the glaciation-related strata within the Upper Ordovician stratigraphic context characterized by shelf clinoforms. The Upper Second Bani Formation is here informally subdivided into lower, middle and upper units. For the detailed log-to-log correlation, see Fig. 12.

Fig. 12. Correlation scheme of five sedimentary logs representatives of the Anti-Atlas deglacial sequence. The four main logs are taken from the glacial trough (Fig. 10); the basinward orientation being to the right. The fifth log to the right relates to an interfluve area, where the thickness of the deglacial succession is minimal. Black arrows show palaeocurrent trends. Letters relate to Fig. 14. Thicknesses in meter. Key to grain size, see Fig. 7.

Fig. 13. The deglacial succession in the Anti-Atlas. (**a**) Overview of the deglacial sequence that onlaps onto older glaciation-related deposits of the lower unit (Tissint section, Fig. 10). It is comprised of a deltaic wedge, ca. 50 m thick, superimposing a glaciomarine wedge, ca. 70 m thick, both constituting the middle unit. The deglacial sequence is truncated by a transgressive sandstone sheet (upper unit). (**b**) The upper part of the sand-rich deltaic wedge in the Aïn Chebi section. A channel fill is underlined. Encircled persons for scale. See figure 12 for location.

Fig. 14. Depositional facies of the deglacial succession in the Anti-Atlas. (**a**) The basal, striated and grooved glacial pavement. B to D: lower unit, E: middle unit, F and G: upper unit. (**b**) Sandstone beds and rippled interbeds in the proximal reaches of grounding zone sediment body. (**c**) Climbing ripples with rhythmic intercalations of muddy drapes, suggesting tidal or day/night cycles in meltwater flows (compass for scale). (**d**) Massive, argilaceous, fine- to medium grained sandstones including a quartz granule (arrow) and intra- to extrabasinal clasts interpreted as ice-rafted debris in a glaciomarine setting dominated by fallout processes from meltwater plumes. (**e**) Laminated siltstones and very fine-grained sandstones, including starved ripples (arrows) in the lower part of the deltaic wedge. (**f**) Cross-stratified sandstones, interpreted as postglacial, transgressive, tidal sandwaves. (**g**) The rapidly fining-upward succession, Lower Silurian in age, at the top the transgressive sandstones, showing HCS beds, waves ripples and intense bioturbation.

Fig. 15. Synthesis of similarities and differences between the Quaternary and end-Ordovician deglacial sequences. Sedimentary logs are scaled while sketches of depositional environments are not. Note

1192 that the GTS in the end-Ordovician case study echoes the GTS characterizing the proximal setting of
1193 figure 8.

Figure 1

Click here to download Figure GSL Fig 1-01.tif

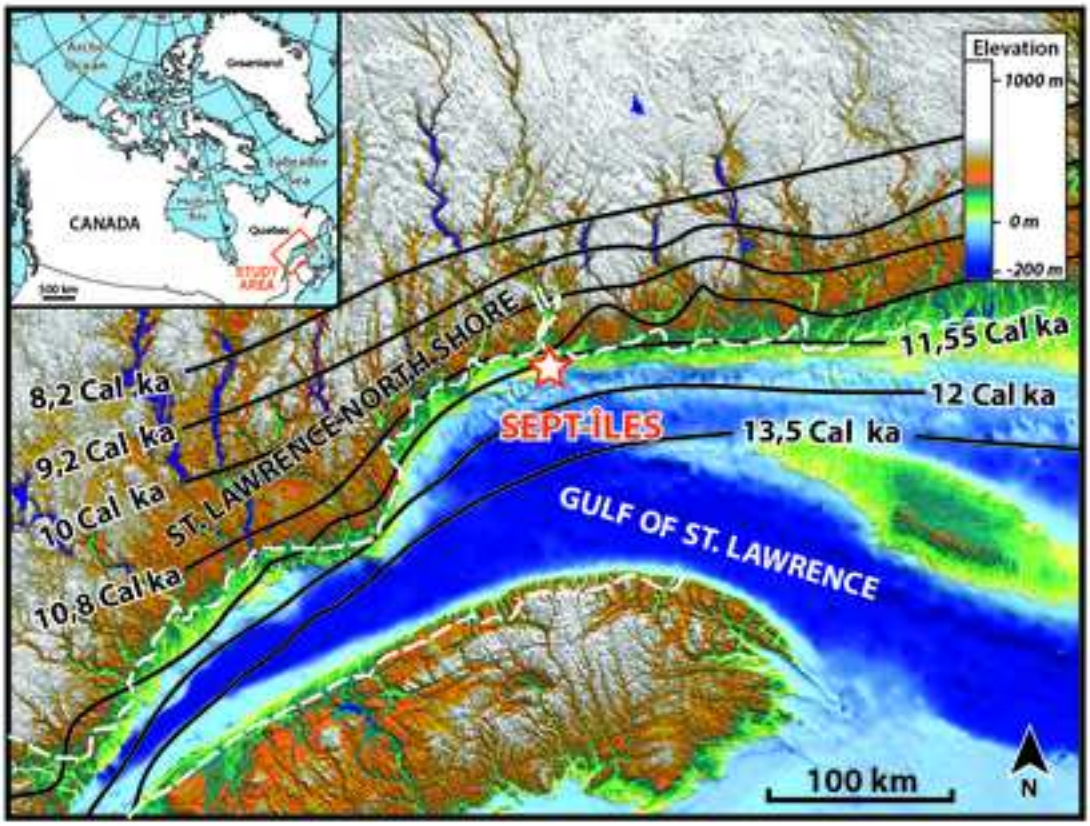

Figure 2

Click here to download Figure GSL Fig 2-01.tif

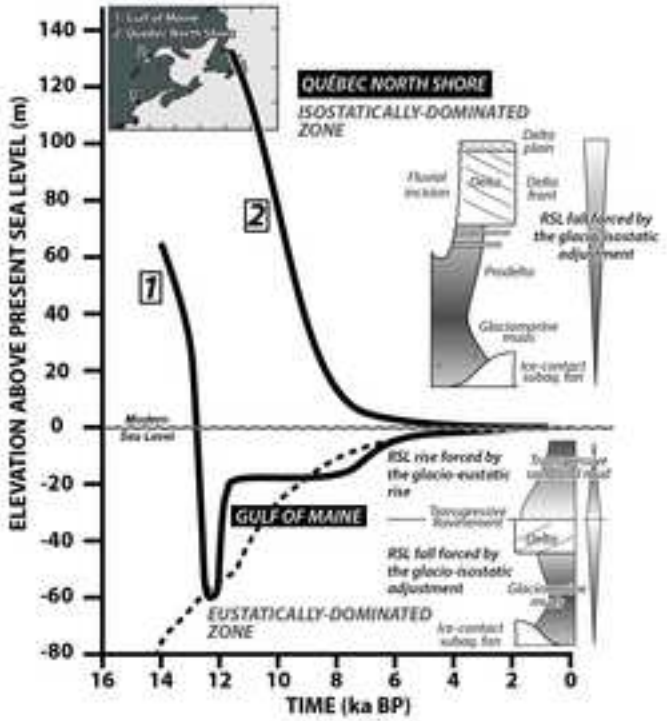

Figure 2

Figure 3

Click here to download Figure GSL Fig 3-01.tif

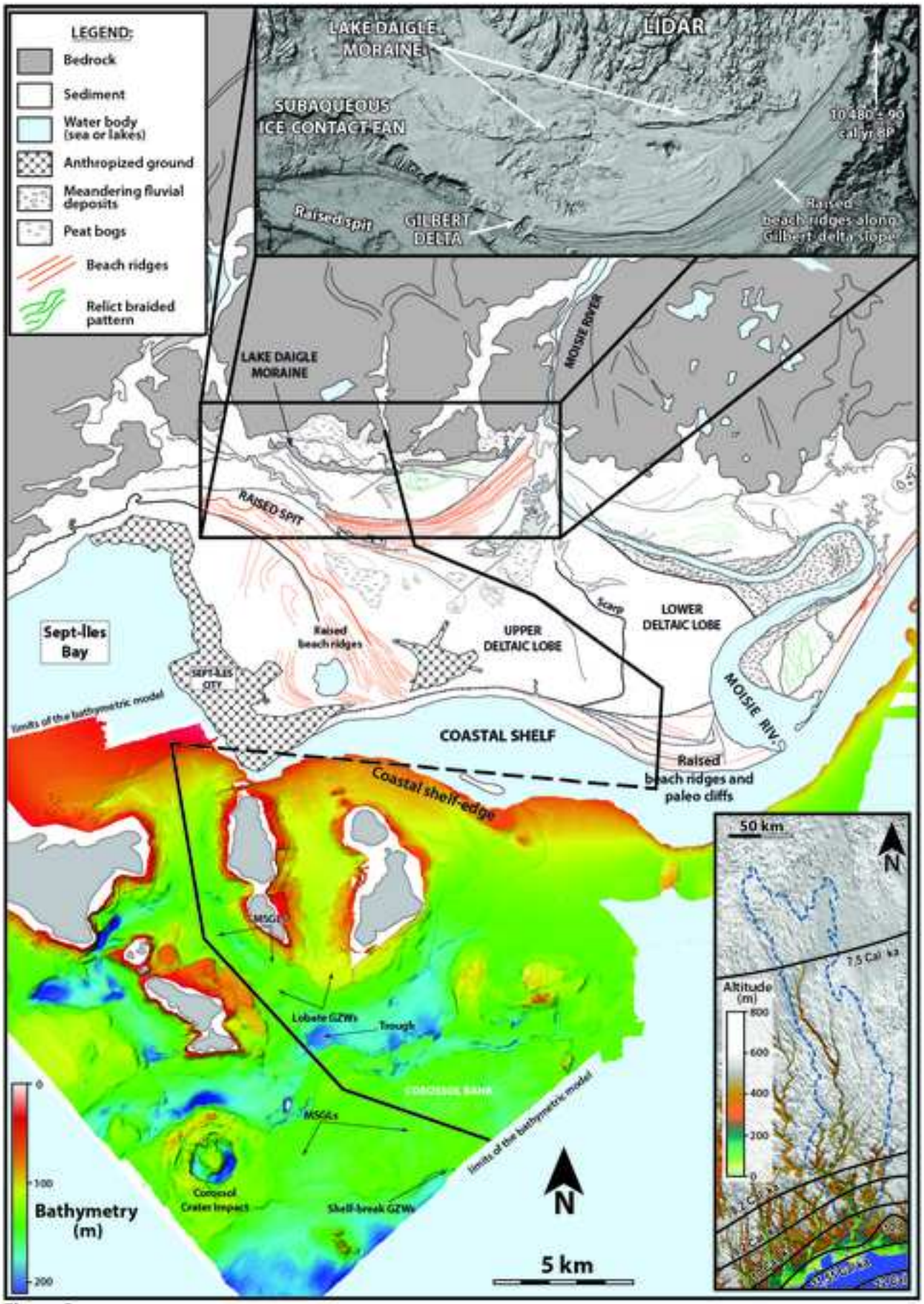

Figure 3

Figure 4

Click here to download Figure GSL Fig 4-01.tif

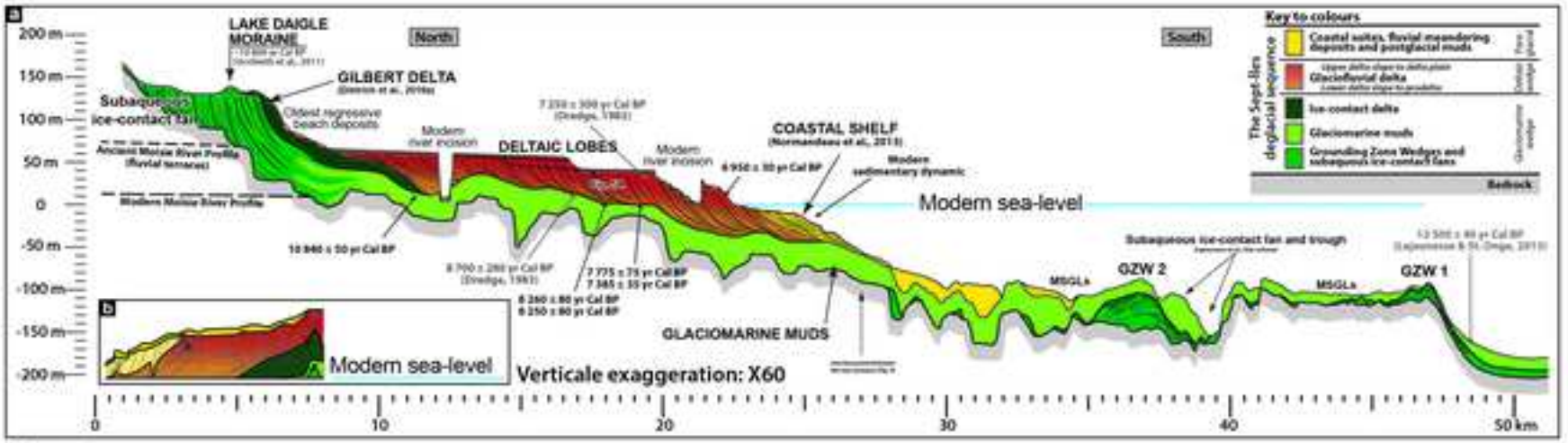

Figure 4

Figure 5

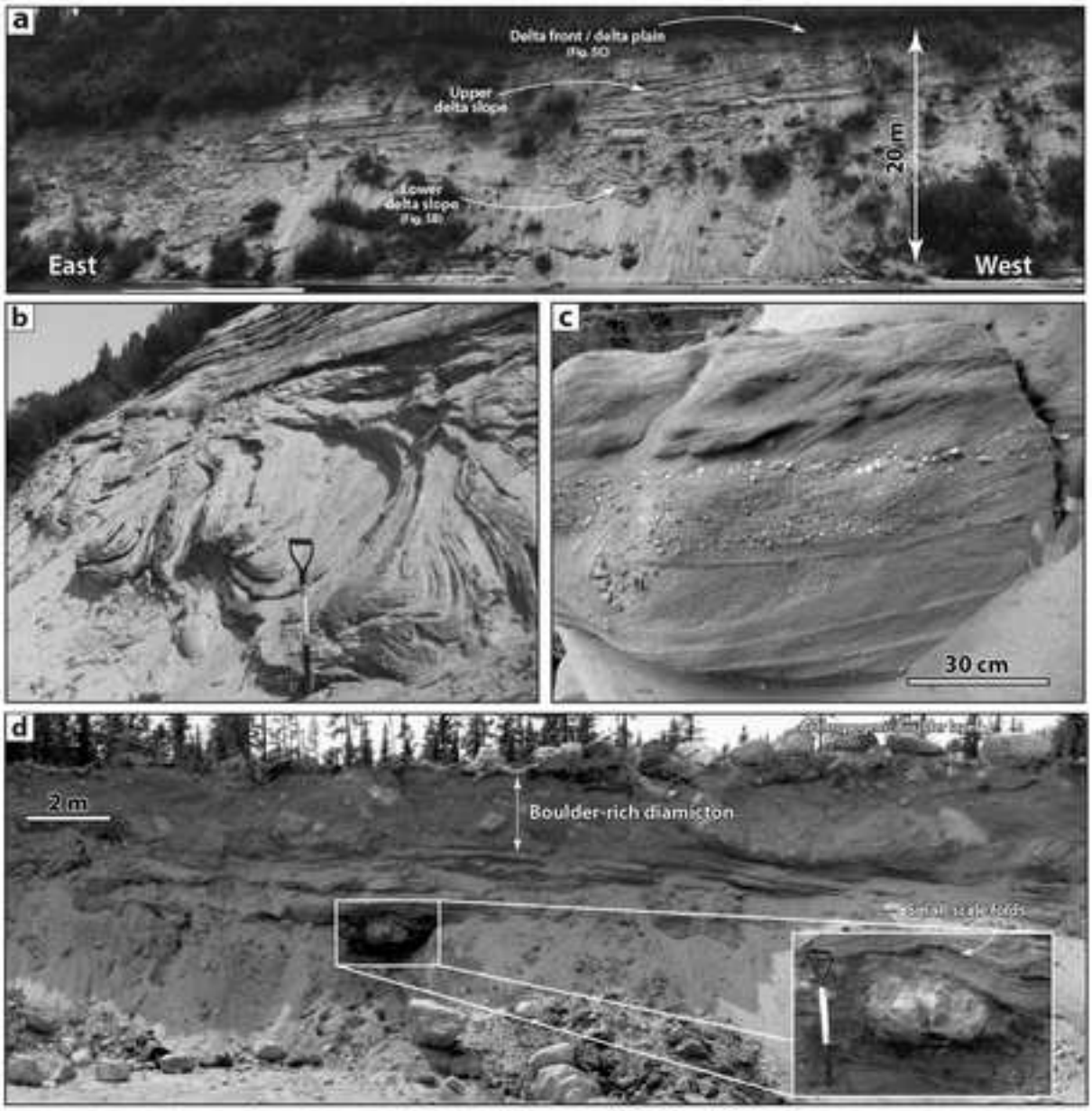

Figure 5

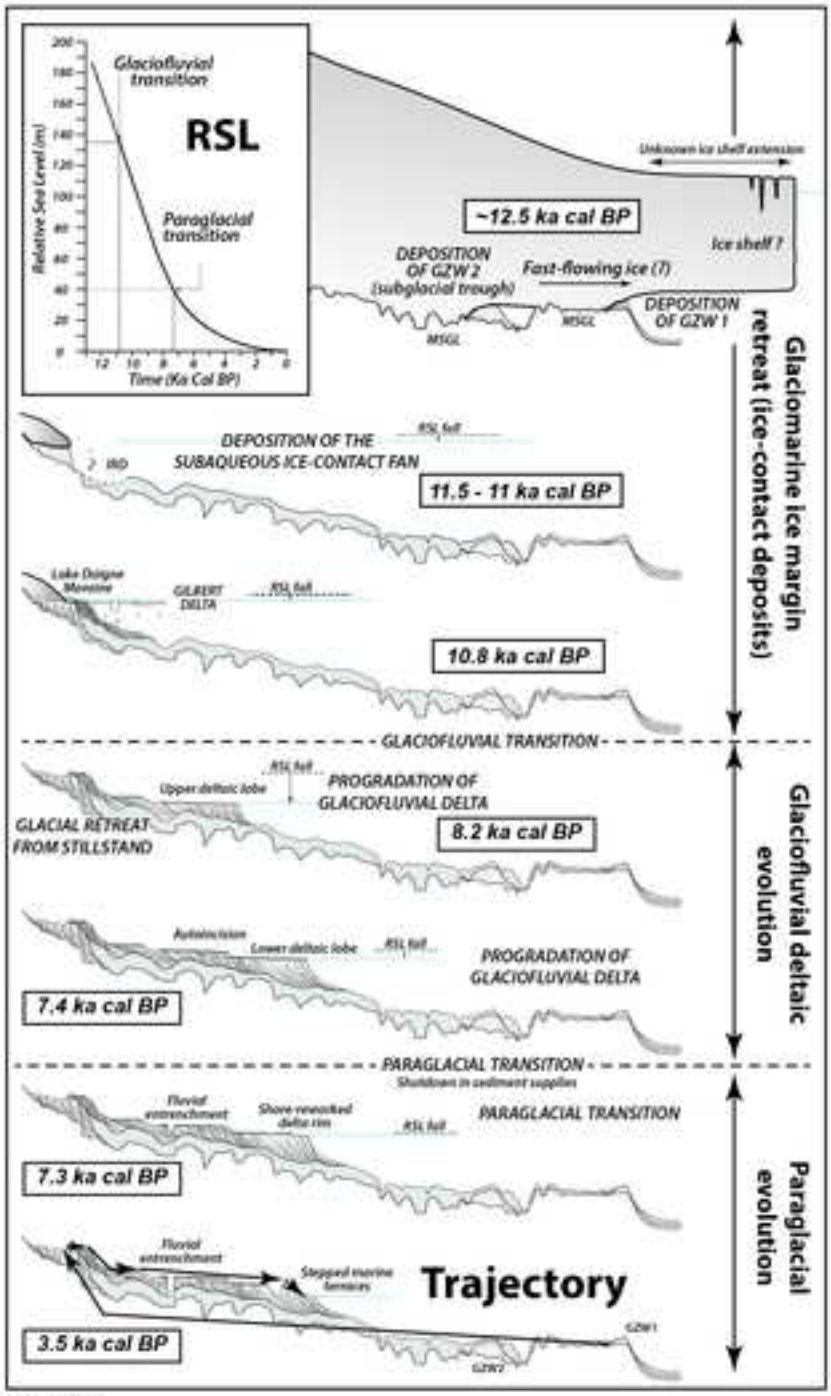

Figure 6

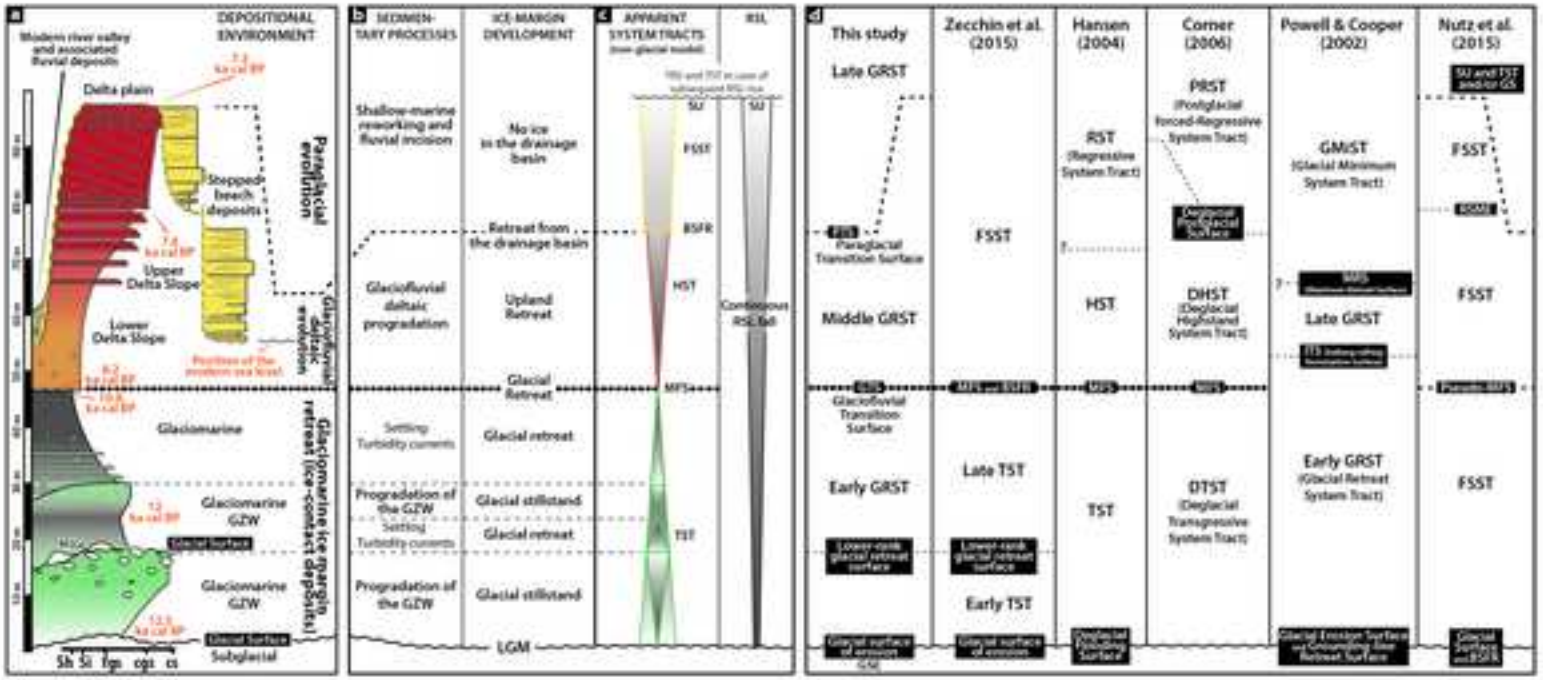

Figure 7

Figure 8 Click here to download Figure GSL Fig 8-01.tif

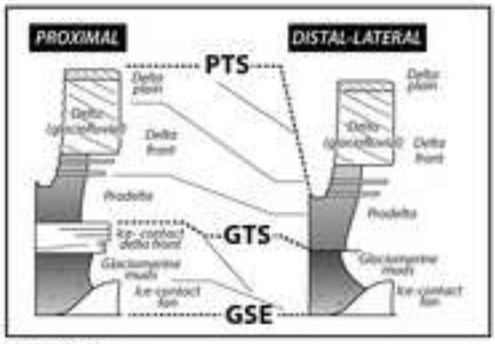

Figure 8

Figure 9

Click here to download Figure GSL Fig 9-01.tif

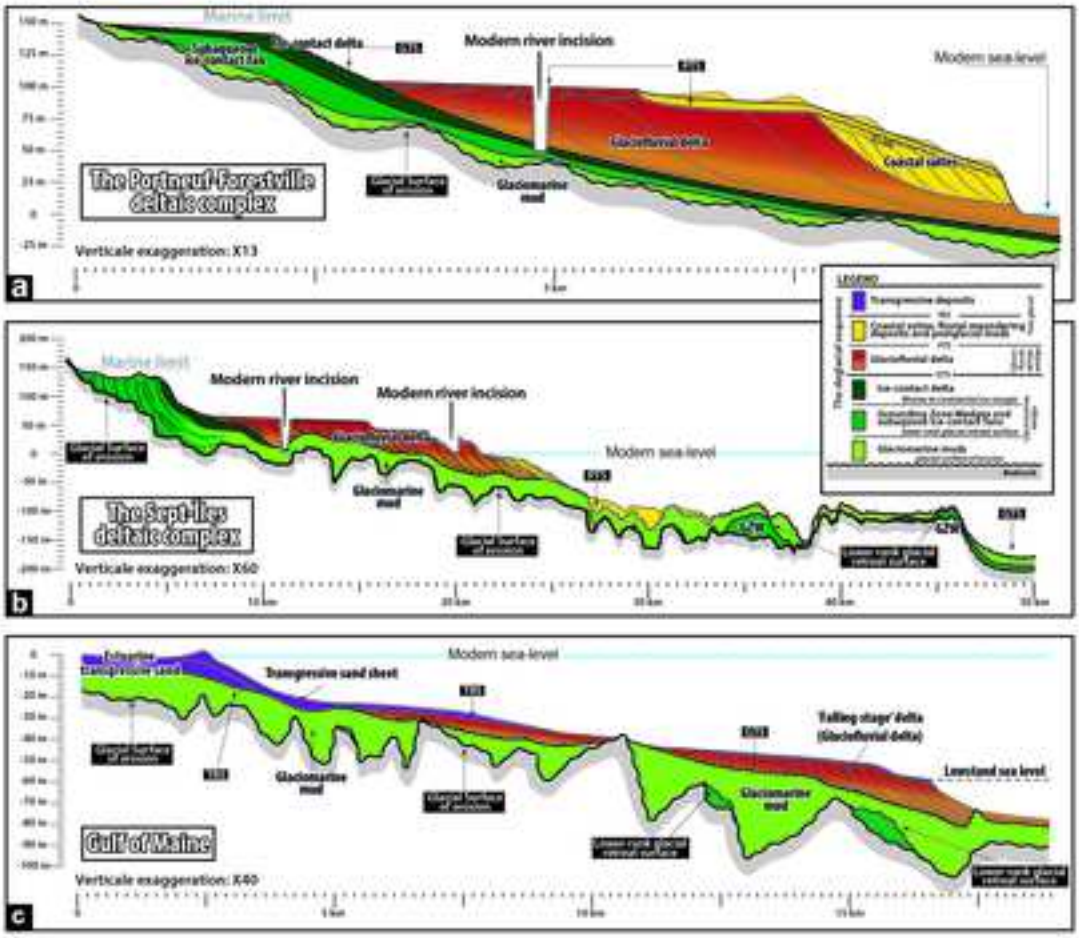

Figure 9

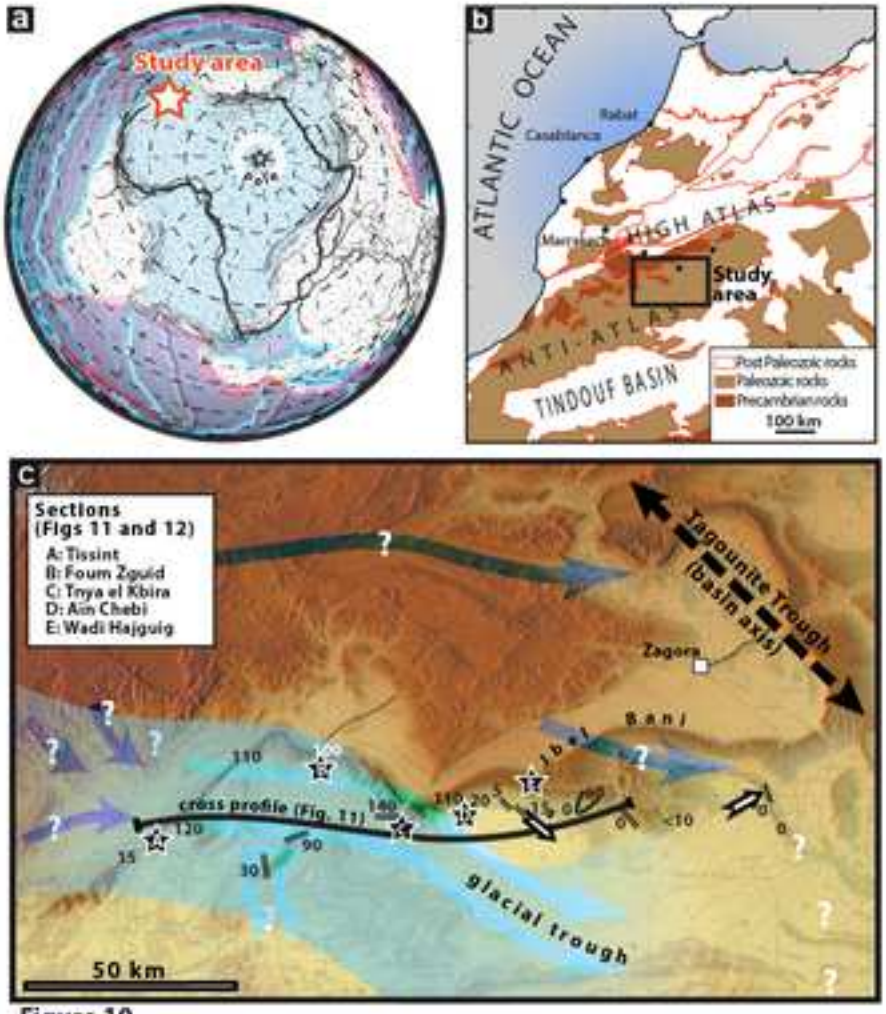

Figure 10

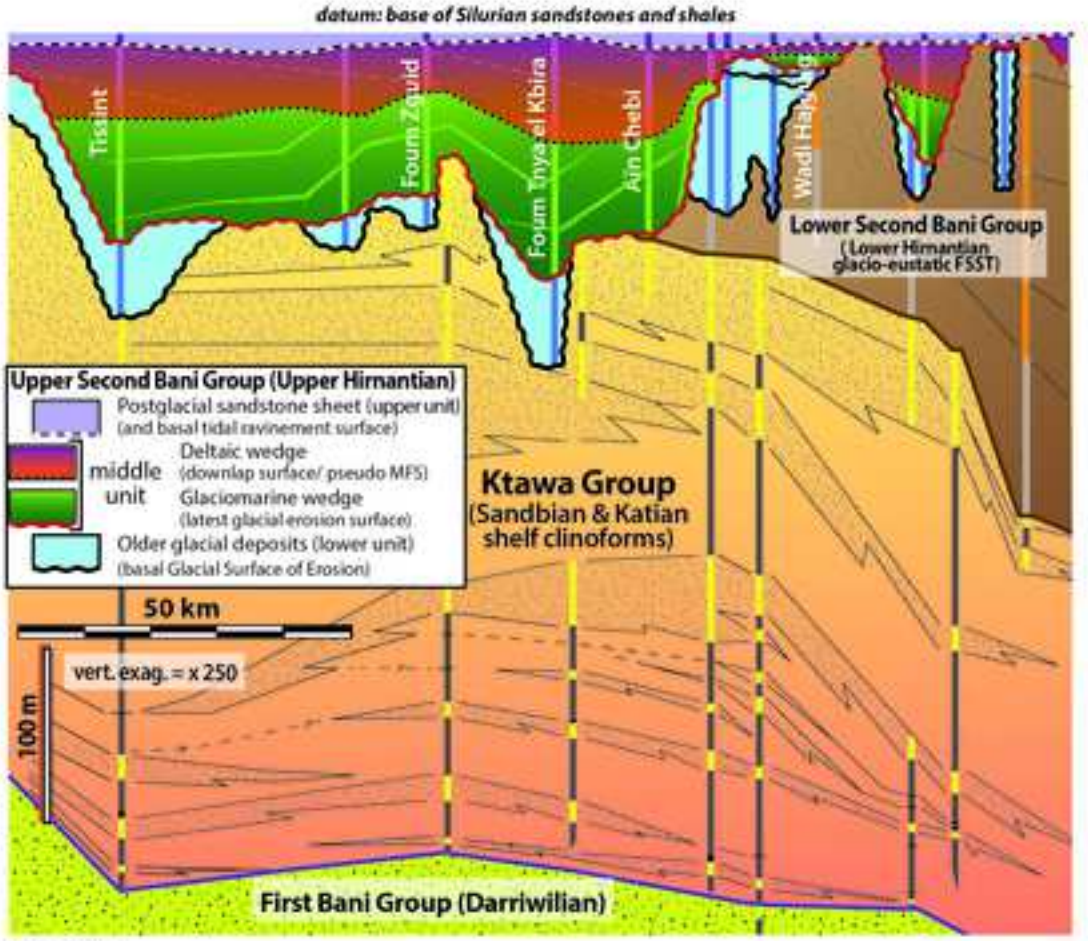

Figure 11

Figure 12

Click here to download Figure GSL Fig 12-01.tif

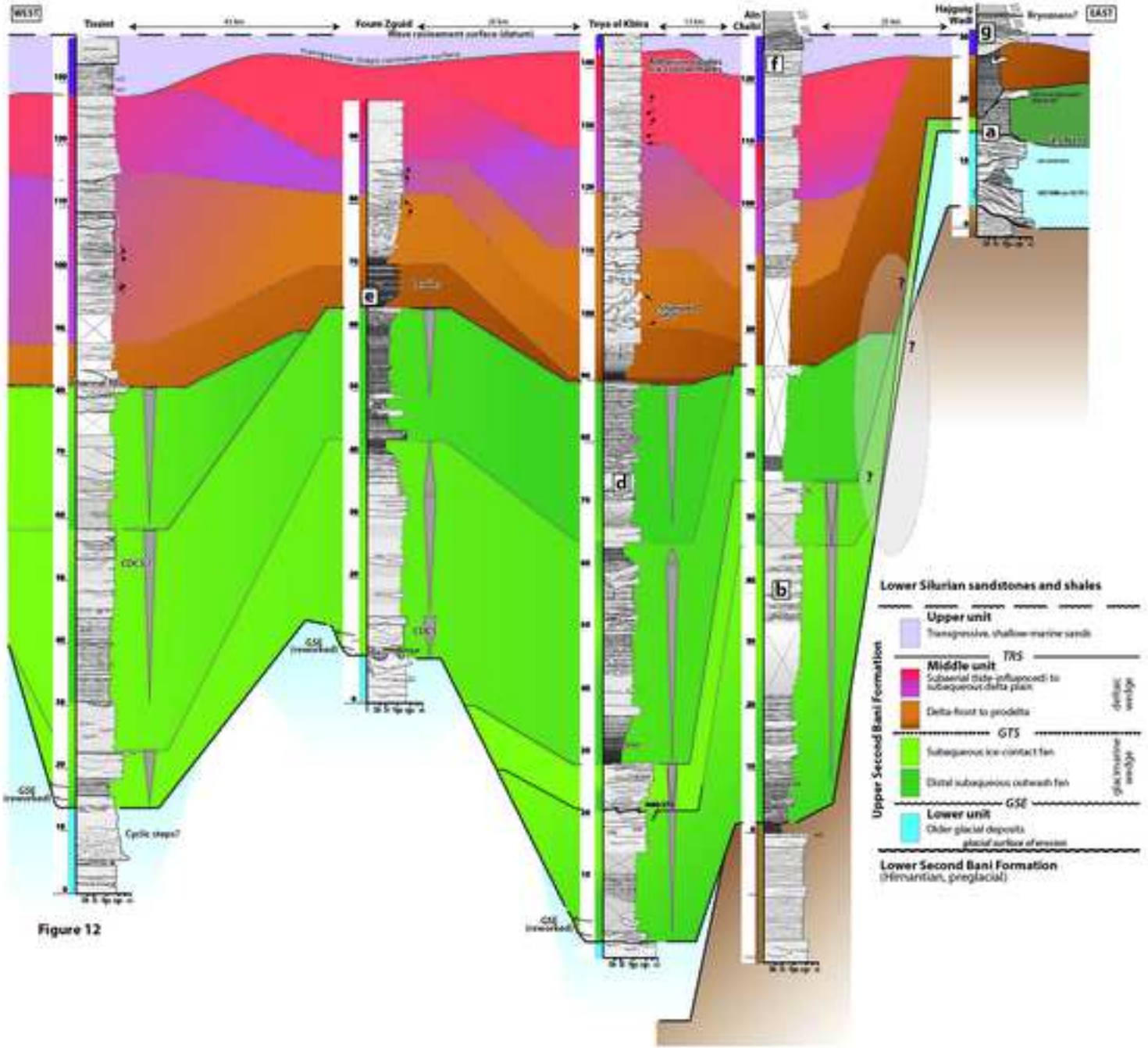

Figure 12

Figure 13

Click here to download Figure GSL Fig 13-01.tif

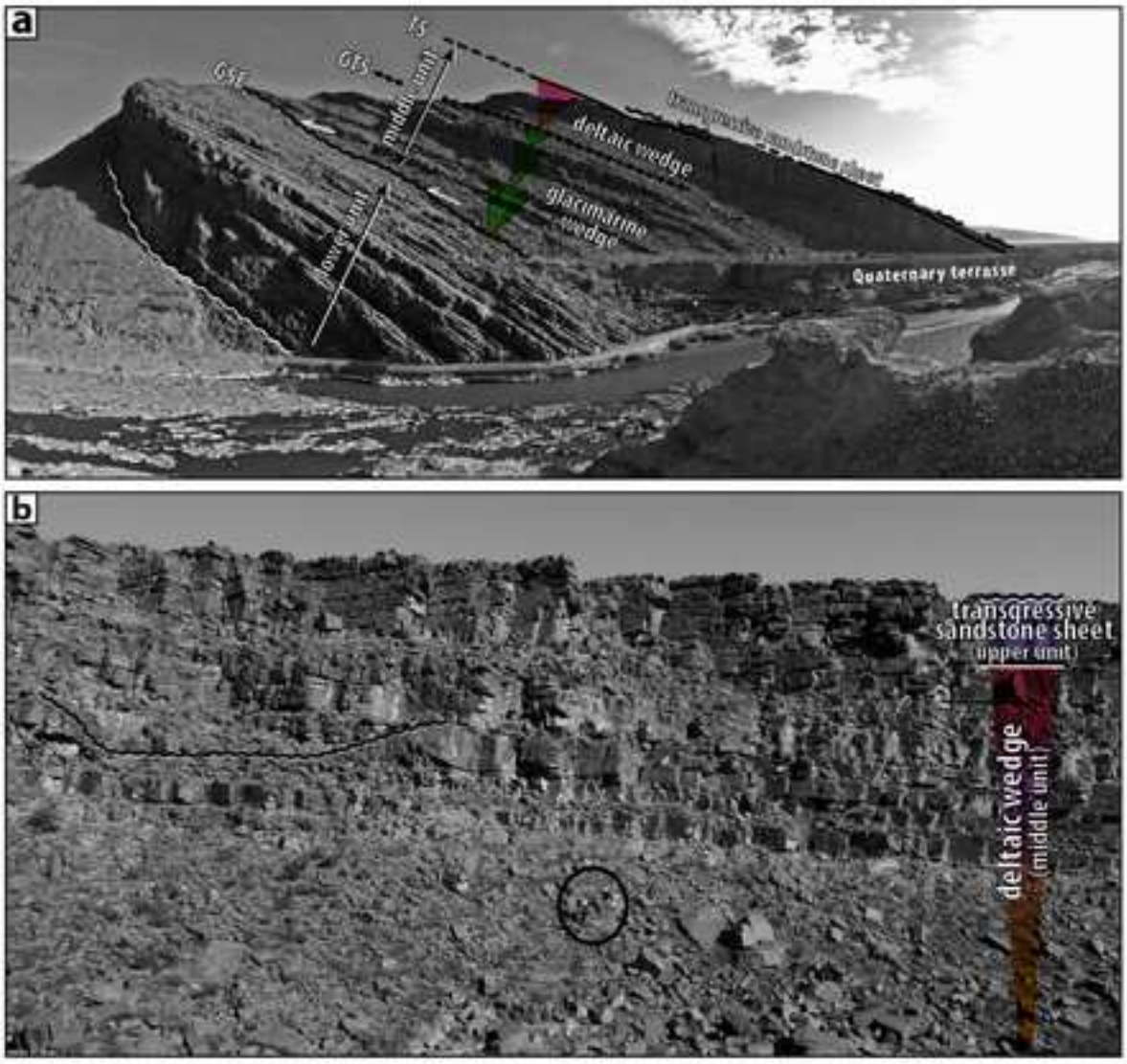

Figure 14

Click here to download Figure GSL Fig 14-01.tif

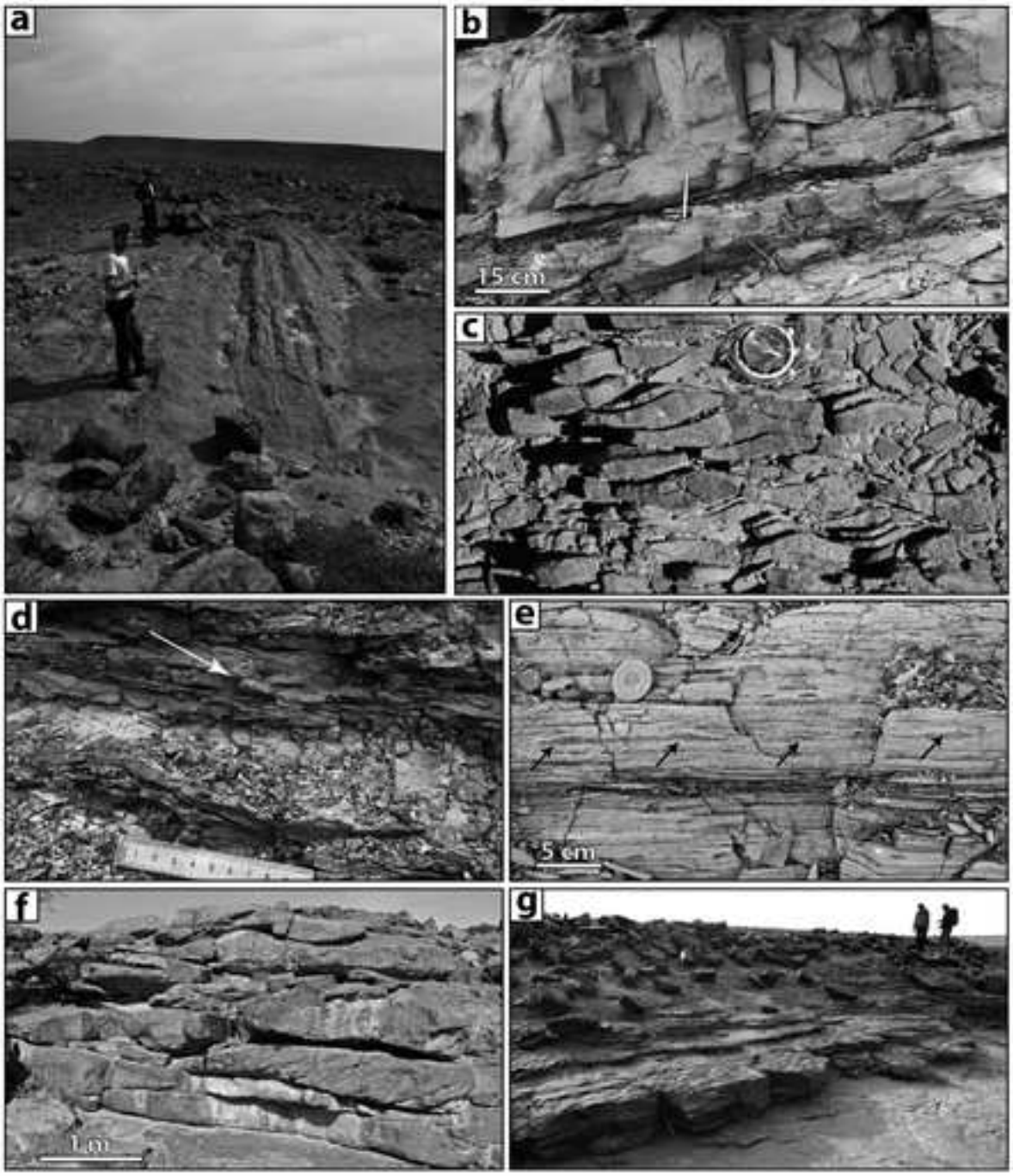

Figure 15

Click here to download Figure GSL Fig 15-01.tif

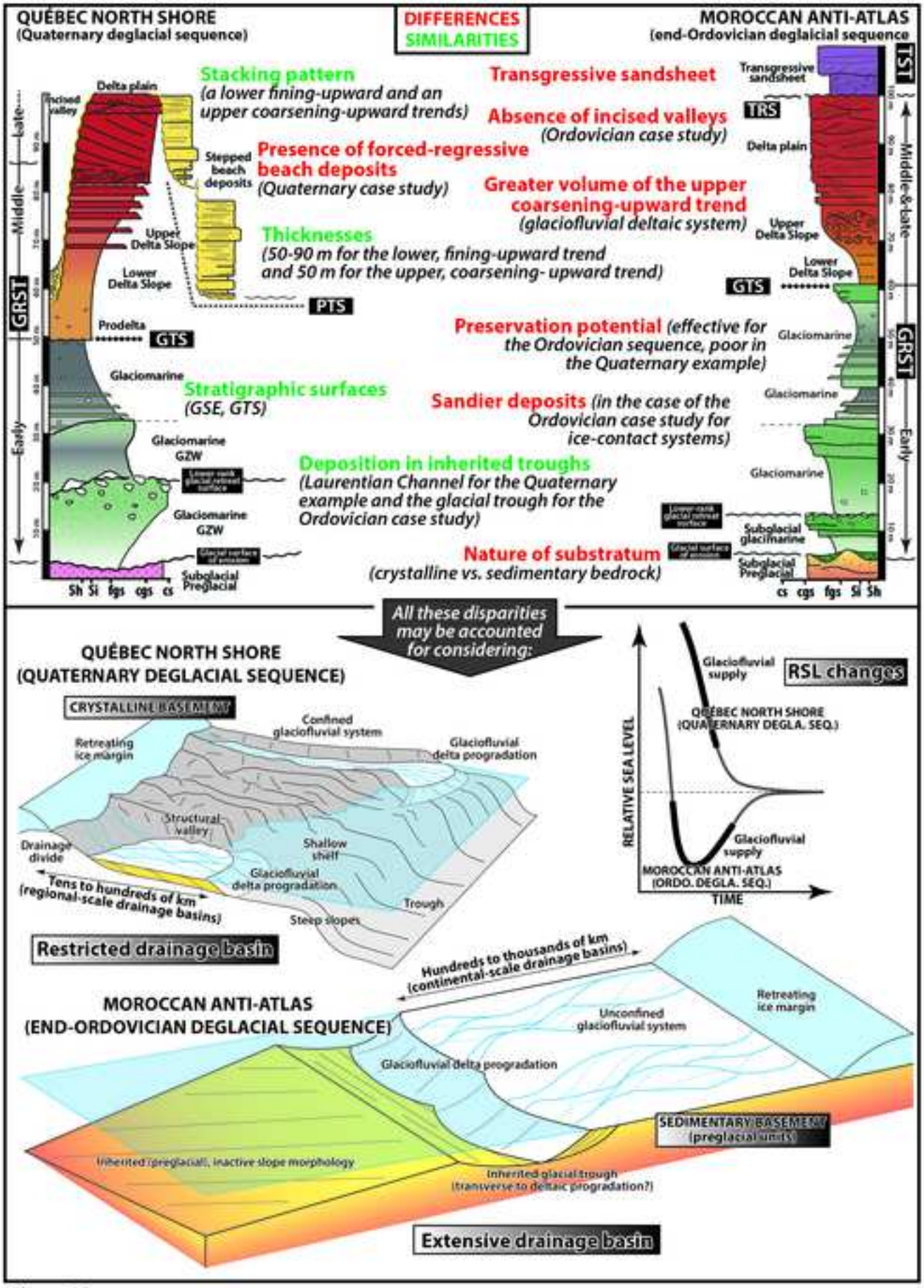

Figure 15